ASSE ACADEMICS PRACTICE SPECIALTY VOLUME 13, ISSUE 2 • 2017

Journal of Safety, Health & Environmental Research

THIS ISSUE

AMERICAN SOCIETY OF SAFETY ENGINEERS • www.asse.org

Journal of Safety, Health and Environmental Research ISSN 2168-1368

Journal of Safety, Health & Environmental Research

Mission: The mission of the *Journal of Safety, Health and Environmental Research* (JSHER) is to peer review theoretical and empirical manuscripts, reviews and editorials devoted to a wide variety of OSH issues and practices.

Scope: As such, JSHER accepts theoretical and empirical papers committed to concepts, analytical models, strategy, technical tools and observational analyses that enhance the decision-making and operating action capabilities of OSH practitioners and provide subject matter for academics. JSHER is an online journal intended to be of interest to OSH academics and to field practitioners concerned with OSH science, emergency and disaster preparedness, fire and homeland security, corporate sustainability and resiliency, economic evaluation of OSH programs or policies, risk-loss control, engineering and other legal aspects of the OSH field.

Submission Guidelines: Each submission to JSHER will be blind peer reviewed by at least two reviewers. Submission of a manuscript to JSHER indicates that the effort expressed has not been published previously and that it is not currently under consideration for publication elsewhere.

Manuscripts that are in agreement with the mission and scope of JSHER should be crafted carefully and professionally written. They should be submitted as an attachment within an e-mail message. Specifically, they should:

- be submitted as an MS Word file(s) with no author identifiers;
- be 8 to 20 double-spaced pages with 1-in. margins all around (approximately 3,000 to 8,000 words including references, but not including illustrations, tables or figures that are not included in the text);
- include a separate document indicating the title, coauthors and the person to whom correspondence should be directed, including that person's name, title, employer, phone number, fax number and e-mail address, and a short (50-word) bio of each author indicating at least the author's current position, highest degrees earned and professional certifications earned;
- include an abstract of no more than 200 words that states briefly the purpose of the research, the principal results and major conclusions, including a short list of key words;
- include a reference section at the end of the manuscript, using APA style to cite and document sources;
- number pages consecutively and clearly indicate new paragraphs;
- document and acknowledge facts and figures;
- present tables and figure legends on separate pages at the end of the manuscript, but indicate where in the manuscript the table or figure should go;
- ensure that graphics, such as figures and photos, are submitted as separate files and are not embedded in the article text;
- for empirical research, at a minimum, the text should include introduction, methods, results and discussion main sections in the text;
- for all submission types, section headers that describe the main content of that portion of the manuscript are advisable.

All submissions should be sent as an MS Word e-mail attachment to:

Sam Wang, Ph.D., P.E., CSP
JSHER Managing Editor
Oklahoma State University
Fire Protection & Safety Engineering Technology
499 Cordell South
Stillwater, OK 74078
Phone (405) 744-5508
qingsheng.wang@okstate.edu

Editorial

It is with great pleasure to summarize four remarkable articles in this issue. The scholars are from organizations around the world, including ExxonMobil Research Qatar; Delft University of Technology, The Netherlands; University of Technology Sydney; University of Alabama; Georgia Institute of Technology; and University of Colorado at Boulder.

The first article, "Hydrocarbon Detection and Quantification Using Autonomous Optical Gas Imaging Technologies," by Hazem Abdel-Moatia, Jonathan Morris, Yousheng Zeng, Martin Wesley Corie II, Yanhua Ruan and Al Sanders from ExxonMobil Research Qatar and Providence Photonics LLC in Louisiana, focuses on identifying fugitive emissions from large scale oil and gas facilities. This article details the development, field testing and qualification of both the IntelliRe and QOGI technologies, and highlights technical challenges and proposed solutions.

In the second article, "A Markov Chain Approach to Domino Effects in Chemical Plants," Nima Khakzad, Mohsen Naderpour and Genserik Reniers from Delft University of Technology and University of Technology Sydney, introduce a methodology based on a Markov chain for modeling domino effects in chemical plants. The application of the methodology is demonstrated via a hypothetical chemical storage plant.

For the third article, "Impact of Design Completeness, Clarity and Stability on Construction Safety Performance," Matthew Hallowell, Anthony Veltri, Christofer Harper, John Wanberg and Sathy Rajendran collaboratively made the first attempt to explore the empirical relationship between various characteristics of project design and safety performance. The implications of findings in this article are that there may also be inherent characteristics of a project design that affect safety performance. These results may encourage practitioners to ensure clarity in design that minimizes disruption and reduces the need for change orders to promote safety and constructability.

The fourth article, "Impact of Discretionary Safety Funding on Construction Safety," is from Siyuan Song, Ibukun Awolusi, Eric Marks and Alexander Hainen at University of Alabama and Georgia Institute of Technology. The objective of this research is to explore the correlation between a construction company's discretionary safety funding strategy and its safety record. Results indicate that increasing discretionary safety funding can improve a company's safety performance.

I hope that you enjoy these articles. As always, I look forward to hearing from you and welcome your future submissions.

Sincerely,

Sam Wang, Ph.D., P.E., CSP
Managing Editor, JSHER

Acknowledgment of Reviewers

The *Journal of Safety Health and Environmental Research* gratefully acknowledges the following individuals for their time and effort as manuscript reviewers during the period between Sept. 1, 2016, and July 31, 2017. Their assistance in raising the standard of the manuscripts published is immense and greatly appreciated. Although the members of the Editorial Board (names are italicized) generally reviewed more manuscripts than others (and provided much additional support), most reviews were handled by ad hoc reviewers, chosen for their unique expertise on the topics under consideration.

Rob Agnew, Oklahoma State University, Stillwater, OK, USA
Ammar Alkhawaldeh, Houston, TX, USA
Michael Behm, East Carolina University, Greenville, NC, USA
JD Brown, Oklahoma State University, Stillwater, OK, USA
Sang Choi, University of Wisconsin-Whitewater, Whitewater, WI, USA
Vic Edwards, Houston, TX, USA
Lina Hall, Chevron, Bakersfield, CA, USA
Joel Haight, University of Pittsburgh, Pittsburgh, PA, USA
Todd William Loushine, University of Wisconsin-Whitewater, Whitewater, WI, USA
Yuan Lu, OXY Oil Co., Houston, TX, USA
Eric Marks, Georgia Institute of Technology, Atlanta, GA, USA
Rachel Mosier, Oklahoma State University, Stillwater, OK, USA
Leslie Stockel, Oklahoma State University, Stillwater, OK, USA
Michael O'Toole, Embry-Riddle Aeronautical University, Daytona Beach, FL, USA
Sathy Rajendran, Central Washington University, Ellensburg, WA, USA
Mitch Ricketts, Northeastern State University, Broken Arrow, OK, USA
Anthony Veltri, Oregon State University, Corvallis, OR, USA
Jan Wachter, Indiana University of Pennsylvania, PA, USA
Steven Zhang, Mustang, Houston, TX, USA
Fuman Zhao, PSRG, Houston, TX, USA

Hydrocarbon Detection & Quantification Using Autonomous Optical Gas Imaging Technologies

Hazem Abdel-Moati[a], Jonathan Morris[b], Yousheng Zeng[b], Martin Wesley Corie II[b], Yanhua Ruan[b] and Al Sanders[b]

Abstract

Identifying fugitive emissions from large scale oil and gas facilities is a time and resource intensive process. Because of limitations of handheld gas detection devices, and the sheer size and complexity of these facilities, smaller leaks may go undetected and unintended releases may occur when plant personnel are not present or the area is unmonitored. Early detection of hydrocarbon leaks using an autonomous system can reduce the risk of conditions that may lead to safety incidents that can result from unintended ignition of gas plumes.

ExxonMobil Research Qatar and Providence Photonics have partnered since 2009 to develop the IntelliRed™ technology. A single-sensor system combines a custom IR imager with a computer vision algorithm to determine the presence of hydrocarbon plumes. A dual-sensor system utilizes two IR imagers with a common optical path and image subtraction techniques to produce a differential image that eliminates background interferences and allows for leak detection while the system is in motion. Quantitative Optical Gas Imaging (QOGI) applies quantitative methods to measure the concentration or emission rate of a gas plume. This article details the development, field testing and qualification of both the IntelliRed™ and QOGI technologies and highlights technical challenges and proposed solutions.

Keywords

Gas release detection and quantification; optical gas imaging; mid-wave IR cameras; autonomous technology; computer vision algorithms; multi-spectral sensors

Leak detection is a fundamental part of safe operations during hydrocarbon exploration, production and processing activities. Hydrocarbon leaks can potentially lead to explosive environments that can result in unintended ignition of gas plumes. In addition, leaks have impacts on processing efficiency and are undesirable from an environmental perspective as hydrocarbons can be precursors for ozone formation and contribute to poor air quality. Hydrocarbon leaks also have an economic impact as they represent lost product. The petrochemical industry devotes considerable resources to leak detection to ensure the safety of workers, protect the environment and maximize production efficiency. Various methods of autonomous leak detection are employed by the petrochemical industry, including catalytic combustible gas detectors, point IR (IR) gas detectors, path IR gas detectors, and acoustic leak detectors. These technologies are mature and provide detection for large hydrocarbon leaks, but early leak detection of small leak rates or fugitive emissions is generally not possible with these legacy technologies.

Handheld flame ionization detectors (FID) are utilized to spot check specific components such as flanges, valves and gauges for small leaks. FIDs are typically used in the U.S. as part of the Environment Protection Agency (EPA) Leak Detection and Repair (LDAR) program. While the handheld FID can detect small leaks, the process is labor intensive and areas that are difficult to access (such as elevated pipe racks or distillation columns) present logistical challenges when using a handheld FID.

The main objective of this article is to highlight the results of 8 years of focused research activities from ExxonMobil and Providence Photonics team of scientists and engineers thatresulted in the development and commercialization of the IntelliRed™ Optical Gas Imaging technology and the Quantitative Optical Gas Imaging (QOGI) technology. The main goals of the research effort were to:

•Develop reliable IR based optical gas imaging technologies that can be used for hydrocarbon leak detection for use in safety applications (e.g., detecting low probability high consequence large scale hydrocarbon leaks before they find an ignition source) and environmental applications (e.g., detecting frequent small-scale hydrocarbon leak sources to improve emissions reduction initiatives).

Hazem Abdel-Moati is the process safety research program lead at ExxonMobil Research Qatar (EMRQ) and has been with ExxonMobil since 2009. He holds a bachelor's and master's degree in Chemical Engineering from Texas A&M University at Qatar. Abdel-Moati was awarded a process safety practice certificate from the Mary Kay O'Connor Process Safety Center and an enterprise leadership program certificate from University of North Carolina's Kenan-Flagler Business School. In addition to his research role, he is the operational safety coordinator for EMRQ. Abdel-Moati received the 2013 Qatar Petroleum HSE Excellence and Innovation Award for the development of the IntelliRed™ autonomous gas detection technology and has five patent applications in the field of optical gas imaging and augmented reality applications, two of which were granted in 2016. He is a member of multiple professional engineering societies and sits on various industrial and academic boards in Qatar. He may be reached at hamoati@gmail.com or hazemm.abdelmoati@exxonmobil.com.

[a]ExxonMobil Research Qatar, Qatar Science and Technology Park, P.O. Box 22500, Doha, Qatar.

[b]Providence Photonics LLC, 1201 Main St., Baton Rouge, LA 70802

•Automate existing IR- based optical gas imaging systems to eventually replace handheld IR cameras and remove field operators from the equation.

•Design hardware solutions that push the boundaries of existing optical gas imaging systems like single-sensor IR cameras (e.g., achieve better resolution, higher frame rates) or come up with completely new designs like the ExxonMobil patented dual-sensor IR camera.

•Develop advanced smart computer vision algorithms that can be integrated with optical gas imaging hardware to accurately detect and quantify hydrocarbon plumes while identifying and filtering out interferences in the background such as moving objects, animals, humans, rain and dust.

•Extend the capability of currently available and newly developed handheld optical gas imaging systems to be able to quantify hydrocarbon plumes.

•Develop QOGI technologies that delivers direct leak quantification (mass emission rate) that will be accepted as an alternative to EPA Method 21 (current method) globally, lowering LDAR costs.

•Field test the systems to evaluate performance and ensure durability and flexibility.

IR optical gas imagers are capable of visualizing hydrocarbon plumes and have become an effective handheld leak detection tool throughout the petrochemical industry. Gas imagers have been approved for use as part of the EPA LDAR program and allow operators to inspect components much more rapidly. Gas imagers provide the ability to detect hydrocarbons remotely, which enables operators to inspect difficult-to-reach areas. The remote nature of the gas imagers also makes it possible to inspect multiple components at one time, providing a significant productivity gain when compared with an FID.

While IR gas imagers provide remote detection capability, they require an operator to view the video and determine whether a hydrocarbon plume is present. The innovation of the IntelliRed™ technology is that it replaces the operator with a computer vision algorithm. Field testing has shown that a single IntelliRed™ system can provide continuous remote leak detection at distances up to 800 ft with leak rates as low as 4 lb/hour.

In the commercially available IntelliRed™ systems, sequential frames from the imager are aligned and the detection algorithm relies on a temporal analysis for detection. The current frame is compared pixel by pixel to a moving average to determine which pixels are changing. Adjacent changing pixels are combined into candidate blobs and their behavior is studied. Features such as speed, direction, size, shape, texture and aspect ratio are used to determine whether the changing pixels are caused by a hydrocarbon plume.

This allows the system to differentiate between a hydrocarbon plume and common interferences such as people and vehicles. In the dual-spectrum versions of IntelliRed™, temporally aligned frames from each imager are compared to determine the presence of a plume and differentiate from other interferences. The design and applications for the single- and dual-sensor IntelliRed™ technologies are presented in this article.

Background

Industrial IR gas imagers are generally passive systems relying on the optical energy emitted by objects in the scene. Absorption bands for most hydrocarbons in the MWIR overlap in a narrow region between 3.2 and 3.4 microns. These imagers typically use cooled MWIR Indium Antimonide (InSb) detectors with a narrow band pass filter to exploit the absorption bands of hydrocarbon compounds. This allows a single imager to detect multiple hydrocarbons, although it does not provide the ability to discriminate between hydrocarbons. Figure 1 shows the absorption band for a compound detectable by these imagers (propane) and a compound nondetectable by these imagers (acetylene) (Stein, Linstrom & Mallard, 2013).

These cooled MWIR handheld IR gas imagers can detect small hydrocarbon leaks. The detection capability is affected by the energy of the background and the absorption characteristics of the target compound. In general, high-temperature backgrounds (such as process equipment) and low-temperature backgrounds (such as sky) provide favorable backgrounds for

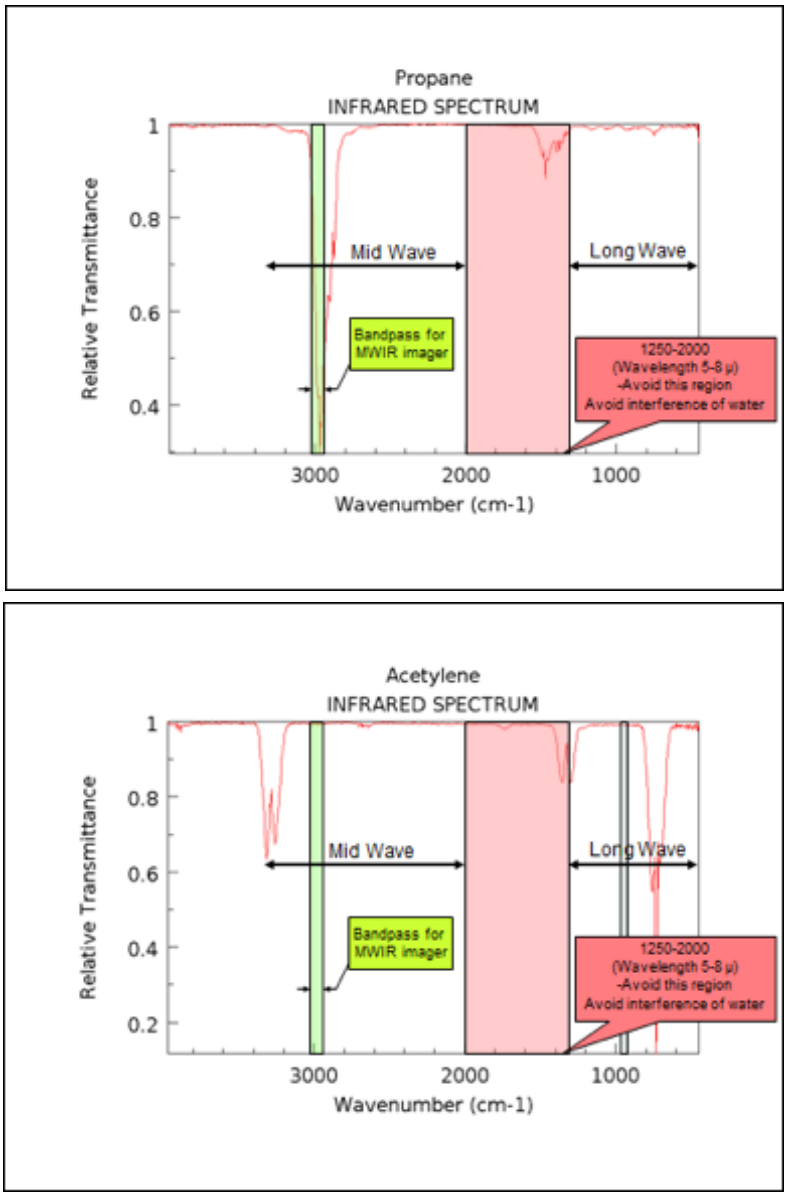

Figure 1: Absorption band for propane and acetylene.

detection. In the case of a warm background, the hydrocarbon plume will absorb a portion of the IR energy and appear as a dark plume in the image. In the case of a cold background, the hydrocarbon plume will emit IR energy at a level higher than the background and the hydrocarbon plume will appear as a white plume against the dark background.

The minimum detected leak rate (MDLR) for a commercially available IR optical gas imager was evaluated in laboratory testing and is reported in Table 1 (Benson, Madding, Lucier, Lyons et al., 2006).

It should be noted that faster optics available in recent cameras result in a larger aperture, more energy to the sensor and higher sensitivity. In turn, this will reduce the MDLR. Correlating these laboratory results to an industrial setting can be difficult as the background temperature and wind conditions are significant variables for the MDLR, as is the distance between the camera and plume.

While most industrial gas imagers operate in the MWIR, it is also possible to operate in the Long-wave IR (LWIR). The boundaries for MWIR (3-5u) and LWIR (8-14u) are generally defined by the strong water vapor absorbance regions. Figure 2 shows the absorbance of water vapor as a function of wavelength. Regions of strong absorbance for water vapor are not suitable for optical gas imaging, as the water vapor in the atmosphere will provide a significant interference.

Compound	MDLR
Pentene	5.6g/hr
Benzene	3.5g/hr
Butane	0.4g/hr
Ethane	0.6g/hr
Ethanol	0.7g/hr
Ethylbenzene	1.5g/hr
Ethylene	4.4g/hr
Heptane	1.8g/hr
Hexane	1.7g/hr
Isoprene	8.1g/hr
MEK	3.5g/hr
Methane	0.8g/hr
Methanol	3.8g/hr
MIBK	2.1g/hr
Octane	1.2g/hr
Pentane	3.0g/hr
Propane	0.4g/hr
Propylene	2.9g/hr
Toluene	3.8g/hr
Xylene	1.9g/hr

Table 1: Minimum detected leak rate.

The primary benefit for using an LWIR imager for optical gas imaging applications is the ability to speciate the compound, provided one has sufficient spectral resolution. In the MWIR, absorbance bands for hydrocarbons are common, meaning a single detector can image multiple compounds but will not be able to speciate. In the LWIR, the absorbance bands spread out allowing the possibility to detect a specific compound or family of compounds. Figure 3 shows the IR spectra of alkanes, alkenes and aromatics.

As shown in Figures 3, absorbance bands for alkanes, alkenes and aromatics that result from the vibration of the carbon hydrogen bonds in most hydrocarbons overlap in the MWIR at about 3.3u. A MWIR imager with spectral filtering to exploit this band will be quite versatile, as it will detect all of the hydrocarbons with absorbance in this region. However, in the LWIR the absorption bands have regions that do not overlap. As such, a MWIR imager cannot speciate or identify specific hydrocarbons, only detecting the presence of a pure hydrocarbon or a hydrocarbon mixture.

A hyper-spectral LWIR imager, on the other hand, can exploit this feature and detect the relative signal of a specific compound. This is difficult to do for the alkanes (e.g., methane, ethane, propane, butane, pentane) due to the poor absorbance in the LWIR; however, it is easier for some alkenes (e.g., propene) or aromatics (e.g., benzene). A hyper-spectral imager operating in the LWIR could be an effective tool for detecting and identifying propene or benzene. In general, the versatility and higher sensitivity of the MWIR imagers make them more suitable for general hydrocarbon leak detection when the target compounds are not known.

Methods

Single-Sensor System Development

The single-sensor IntelliRed™ technology comprises a lone MWIR sensor mated with a custom continuous zoom 25mm to 100mm lens with an optional 2X optical doubler that extends the focal range to 200mm. This optic can be remotely zoomed and focused, enabling a single camera installation to monitor various objects at different distances.

At the heart of the single-sensor technology is the computer vision algorithm that processes the video stream from a single IR optical gas imager. The detection algorithm analyzes sequential frames from the IR video to detect a hydrocarbon plume and generate an alarm. Early versions of the detection algorithm utilize an analog 8-bit 320 x 240 resolution video stream. The analog video was encoded and transmitted wirelessly to a server running the detection algorithm. Later versions utilized an 8-bit and a 14-bit 640 x 512 stream. Figure 4 (p. 350) describes the steps of the computer vision algorithm.

The first step for the detection algorithm is to pre-process the video stream. This process includes contrast enhancement using histogram equalization and de-noise using a bilateral smoothing filter. The enhanced image is then registered to the previous frame. The detection algorithm studies the changes in pixels over time, so it is important to register each frame prior to processing.

Hydrocarbon plumes vary in shapes and sizes and are in con-

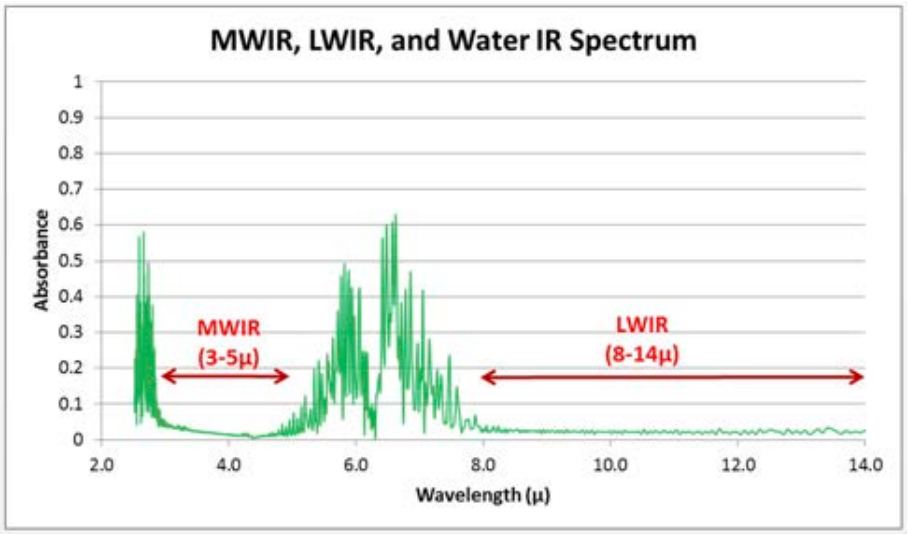

Figure 2: MWIR, LWIR and water IR spectrum.

stant movement once they escape from the release source. The plume is never static and the molecules are always in motion, as they need to encounter an environment with a temperature close to zero degrees kelvin to remain static, which is nearly impossible to achieve outside lab conditions. The IR camera and the computer vision algorithm utilize this physical characteristic of hydrocarbon plumes released into the environment to successfully register and track the releases.

Techniques employed to achieve registration and stabilization include feature point extraction using Shi-Tomasi corner detector and associating pairs of feature points using Pyramidal Lucas-Kanade optical flow method (Zeng, Zhou, Katwala & Calhoun, 2006). In addition, affine transformation modeling is implemented to fit the geometric changes between image frames utilizing random sample consensus (RANSAC) to remove outliers. The registration process can be enhanced by using edge detection (Canny edge detector) to mask edges in the scene and reduce noise due to improper registration. The result from utilizing these techniques is a series of frames with improved contrast and good spatial registration.

Once the image has been registered, the algorithm will compare the current frame to a moving average of the background. An intensity threshold is applied to determine which pixels are changing relative to the moving average. This process reduces the image to binary data, with each pixel classified as changing or not-changing. Adjacent changing pixels are then grouped to form blobs and additional spatial thresholds are applied to the candidate blobs.

The blobs are subjected to minimum and maximum sizes (in terms of pixels). The minimum blob size threshold removes noise in the image, while the maximum size threshold removes blobs caused by dramatic changes in scene intensity which affect most pixels (such as occurrences when a cloud moves to reveal direct sunlight). A bounding box is drawn around candidate blobs and thresholds are applied to the aspect ratio of the bounding box (height versus width) as well as the fill ratio of the bounding box (ratio of pixels inside the box which are changing to those which are not changing). If a candidate blob survives these spatial filters, it is considered to be a foreground object and it is associated with blobs from previous frames using Global Nearest Neighbor (GNN) technique. If it does not survive the spatial filters, it will be classified as a background object and is not considered for subsequent processing.

A track is established for each foreground object to track the movement across multiple frames. A blob is associated with an existing track by comparing the location of the center of the bounding box with the most recent blob in the existing tracks. Thresholds are applied to limit the acceptable distance between the current blob and the previous blob in an existing track. A second threshold is applied to limit the acceptable distance between

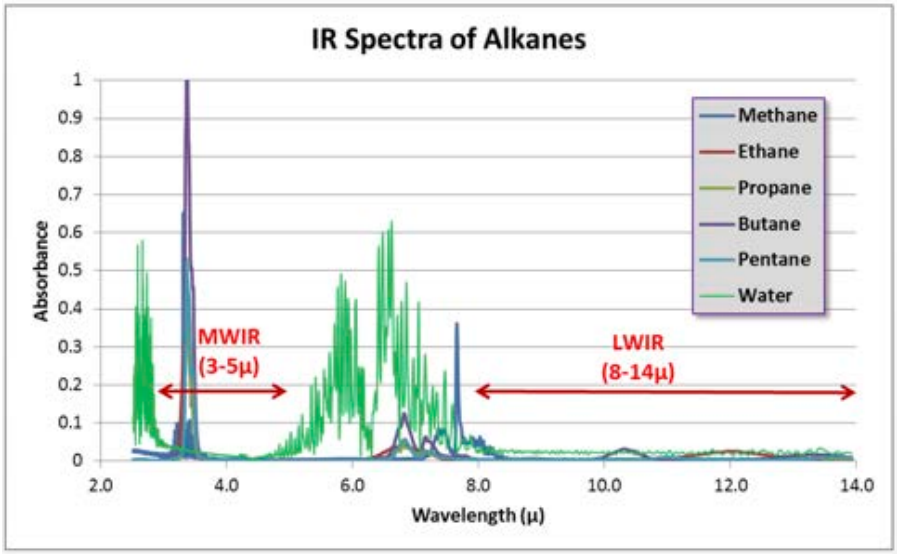

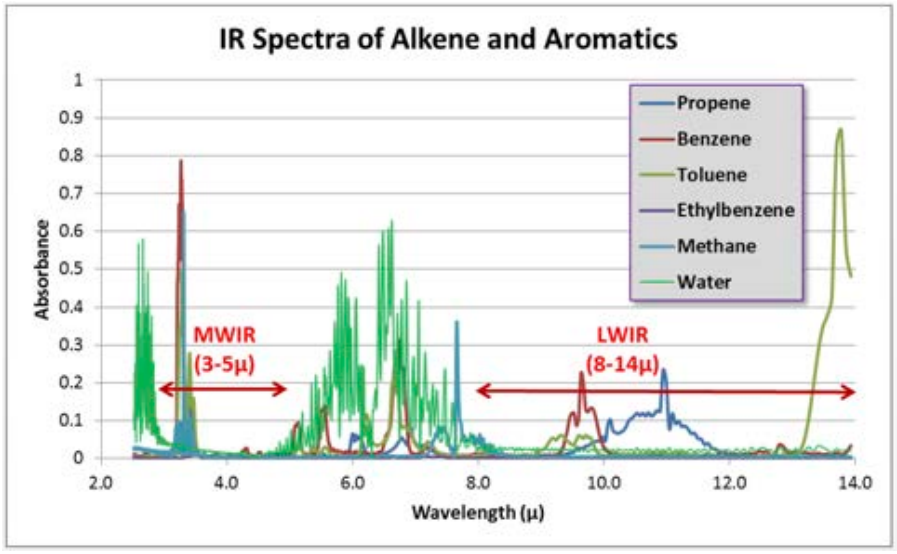

Figure 3: IR spectra of alkanes, alkenes and aromatics.

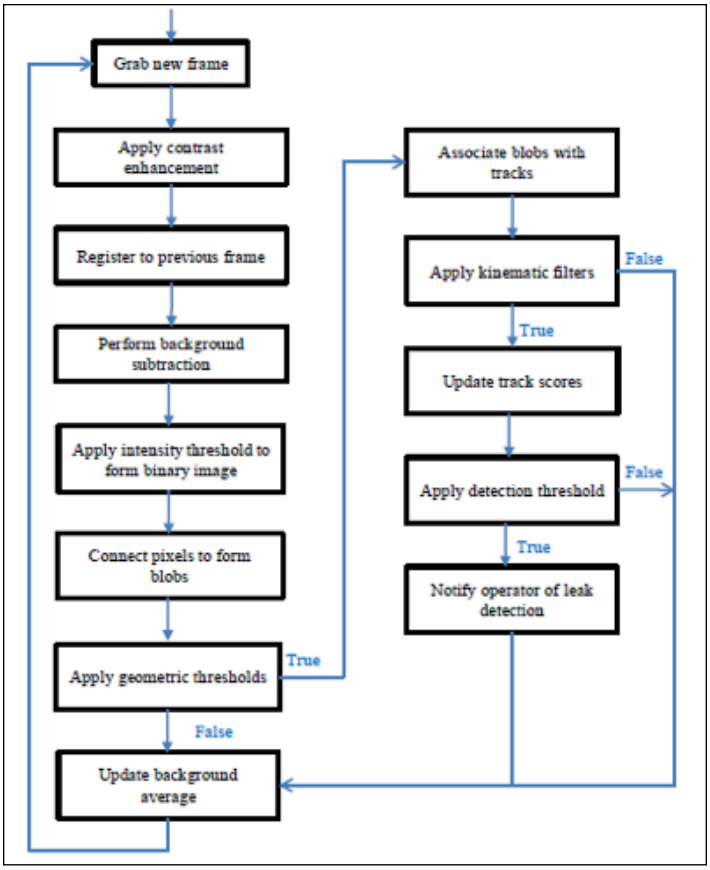

Figure 4: IntelliRed™ detection algorithm.

the current blob and the origin of an existing track. If the blob cannot be associated with an existing track, a new track is established for the blob in the current frame for subsequent processing. The detection algorithm is capable of monitoring hundreds of tracks simultaneously.

Once the blobs are segmented into tracks, each track receives a score which describes the likelihood that the track represents a plume. A blob can increment the score of the track if it passes additional filters. The distance traveled between the current blob and the previous blob is used to calculate an average speed for

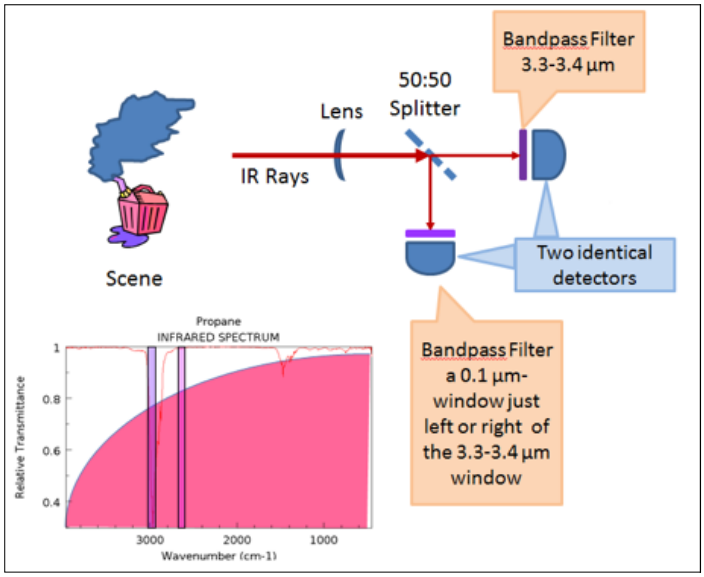

Figure 5: IntelliRed™ differential infrared optical design.

the track. If the track represents a collection of blobs which is relatively static it is not likely to be a plume (more likely to be a person). Similarly, if the average speed of the track is relatively high, it is not likely to be a plume (more likely to be a vehicle). These thresholds are correlated to the distance between the camera and the scene and are typically very loose.

One critical threshold to filter out nongaseous blobs is the degree to which the blob is changing shape relative to previous blobs in the track. The algorithm describes the shape of the blob using a combination of the first-, second- and third-order moments. Moments of a blob can be used to uniquely describe the information contained in the blob. The lower-order moments represent some well-known fundamental geometric properties of the image. For example, zero-, first- and second-order moments represent ,respectively, the area, the mass center of the blob and the orientation of the principal axes of the blob. While there are other shape comparison methods available (such as blob correlation and blob matching), the algorithm uses moments because they are fast to compute.

Once the blobs have been processed and track scores have been updated, the moving average of the background is updated. Foreground objects and background objects both influence the moving average but at different rates. A background object will typically influence the background moving average at a higher rate than the foreground objects. The rate at which foreground and background objects update the moving average can be adjusted dynamically by the algorithm. For example, the conditions of the scene may set the weight of background objects to 5% (meaning the current frame counts 5% towards the new average value while the previous frames count 95%) and the weight of foreground objects to 1%. This approach allows the algorithm to adapt to a changing scene as a foreground object that becomes stationary will eventually become part of the background, such as occurs when a vehicle drives into the scene and stops.

A final threshold is applied to the score for each track. When the track score exceeds this threshold the algorithm declares that a plume has been detected. The location of that confirmation is recorded and the scores are reset. Depending on the sensitivity settings on the algorithm, a notification may be sent immediately or multiple confirmations may be required before notification. The nature of the notification can be an e-mail (with an embedded still image of the leak), fax, multimedia text message, analog voltage, analog current, or Modbus TCP alarm.

The detection algorithm utilizes multiple thresholds to achieve detection. Some of these thresholds can be set during installation of the camera, such as those related to the distance between the camera and the objects which are monitored. Other thresholds must be set dynamically by the algorithm in response to changing factors in the scene. For example, at night, energy levels in the scene tend to decrease so the intensity threshold applied to changing pixels needs to be lowered. Still other thresholds trade-off detection sensitivity with the false alarm rate and can be set by the user, such as the confirmation score for a track. The combination of these thresholds allow for the deployment of a complex detection algorithm to a variety of environments, providing continuous autonomous remote leak detection capability.

One limitation of the current single-sensor IntelliRed™ technology is that the temporal analysis requires careful alignment

of sequential frames from the imager. A step-and-stare inspection technique covers a large field of view with a series of automated steps, with the imager remaining stationary at each step. If the imager is moving or shaking during detection, then the frames must first be aligned using registration techniques prior to detection. These frame alignment techniques can be resource intensive and generally require several high contrast features in the image.

Figure 6: IntelliRed™ differential infrared frame.

Another limitation of the current single-sensor technology is that certain interferences can be difficult to filter out. For example, a steam plume will present a signal in a MWIR imager that behaves in a manner similar to a hydrocarbon plume. One effective technique to distinguish between steam and hydrocarbon is to use the plume's polarity. A steam plume consists of water droplets that are generally at a higher temperature than the background and, therefore, the plume appears white in an IR image. A hydrocarbon plume generally absorbs a portion of the energy from the background and appears darker than the background. This simple polarity test is effective, but a more robust filter is provided by the dual-sensor IntelliRed™ technology (DIR) currently undergoing qualification.

Dual-Sensor System Development

The working principle of the IntelliRed™ DIR camera is illustrated by Figure 5. The IR energy coming from a scene is reimaged onto a beam splitter positioned in the optical path. As a result, a portion of the IR energy from the scene passes through the splitter to reach one MWIR detector and a portion of the IR energy from the scene is reflected to the second MWIR detector.

This beam splitter can be a simple broadband splitter with reflectance and transmittance of approximately 50%. This design evenly splits the energy with approximately 50% reaching each detector. Alternatively, the splitter can be dichroic allowing for wavelength specific reflectance and transmittance. Careful design of the spectral filtering and dichroic splitter can provide each detector with nearly 100% of the energy in its respective wavelength.

The unique feature of the dual-sensor design is that the specific wavelengths selected for the bandpass filters make one detector sensitive to hydrocarbon plumes while the second detector is not. The detector sensitive to hydrocarbon gas operates with a bandpass filter in the 3.3u to 3.4u range and is referred to as the gas band (GB) imager. The second detector is referred to as the reference band (RB) imager and has a bandpass filter that is shifted to the right or left of the GB imager. Since the RB imager is still operating in the MWIR region, it provides a spatially and temporally registered reference image that is very similar to the GB but insensitive to hydrocarbon gas. Figure 6 shows the raw unprocessed data from a single frame of a dual-sensor imager.

The left side of the image in Figure 6 shows the GB imager and the right side shows the RB imager. Notice the presence of a hydrocarbon plume in the GB image and the absence of the plume in the RB image. Other interferences, such as people and steam, are present in both images. In a simple sense, a pixel-by-pixel subtraction will reveal the presence of a hydrocarbon plume. In reality, more complex processing is required but field testing has shown that this design can achieve autonomous detection within a single frame. With single frame detection, new applications such as aerial pipeline surveys are now possible. The hydrocarbon plume represented in this image was generated by a propane leak at the rate of 1.5 lb/hour and imaged from a distance of 300 ft.

Quantitative Optical Gas Imaging Technology Development

EPA has promulgated regulations governing the detection and repair of equipment leaks that cause fugitive emissions of volatile organic compounds (VOC). These regulations are embedded in various emission standards and are generally referred to as LDAR programs. Similar regulations exist for many regions globally, with associated LDAR surveys being performed regularly in these regions (including Europe).

Two primary methods for LDAR surveys are currently being used: sniffing (Method 21) and optical gas imaging (OGI). Method 21 was developed decades ago when there was no better method. It has been effective in reducing VOC emissions reductions though the method contains significant uncertainties and is very labor intensive. In addition, it is the primary method used currently in the U.S. to detect leaks (EPA, 2014). Method 21 requires operators to use portable instruments, typically an FID or a photon ionization detector (PID), to "sniff" around the circumference of individual equipment components (e.g.,, valves, flanges, pump seals). If the detector reading (ppm) is higher than target thresholds, the component is deemed to be leaking and it must be repaired within a certain time.

Fugitive VOC emissions from a facility are calculated based on the ppm readings (referred to as screening values or SVs) and empirical correlations between SVs and mass emission rates (EPA, 1995). Because the leak check is performed on each individual component basis, the implementation of a Method-21-based LDAR program is tedious, labor intensive and prone to errors due to amount of recordkeeping associated with thousands to hundreds of thousands of components that must be tracked.

OGI emerged as a viable alternative to Method 21 about 10 years ago. Detecting VOC leaks using OGI is more efficient than Method 21 because leak checking using OGI is visual, making

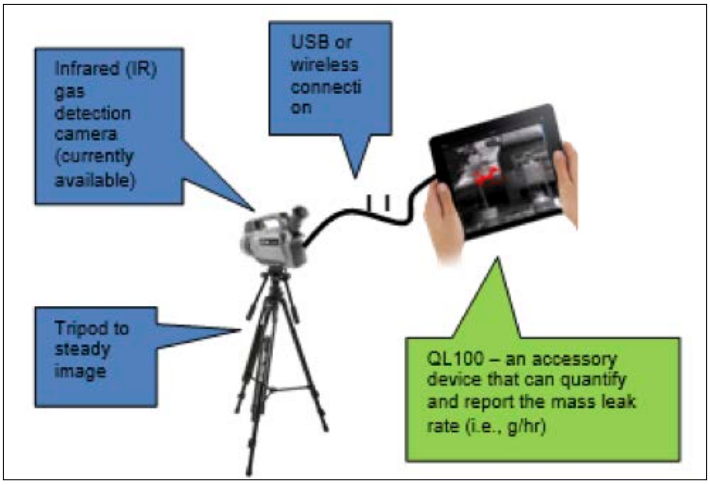

Figure 7: QOGI technology

detection faster, and it can be performed over an area instead of component-by-component. For this reason, the OGI method is also referred to as "smart LDAR."

In December 2008, EPA promulgated the Alternative Work Practice (AWP) rule allowing operators to use OGI for LDAR compliance. However, the AWP rule requires operators to continue to perform leak checks using Method 21 at least once a year. The reason is that OGI offers high productivity but to date has provided a qualitative result only with estimate of leak rate. This is one shortcoming of OGI from a regulatory perspective, thereby hindering its adoption as a true alternative to Method 21. The advent of QOGI allows the operator to quantify the mass leak rate from the captured video images (Figure 7). Existing OGI camera technology is the basis for the new QOGI technology. If an OGI camera detects a leak, then the operator can apply the new QOGI technology to quantify the mass leak rate from the captured video images.

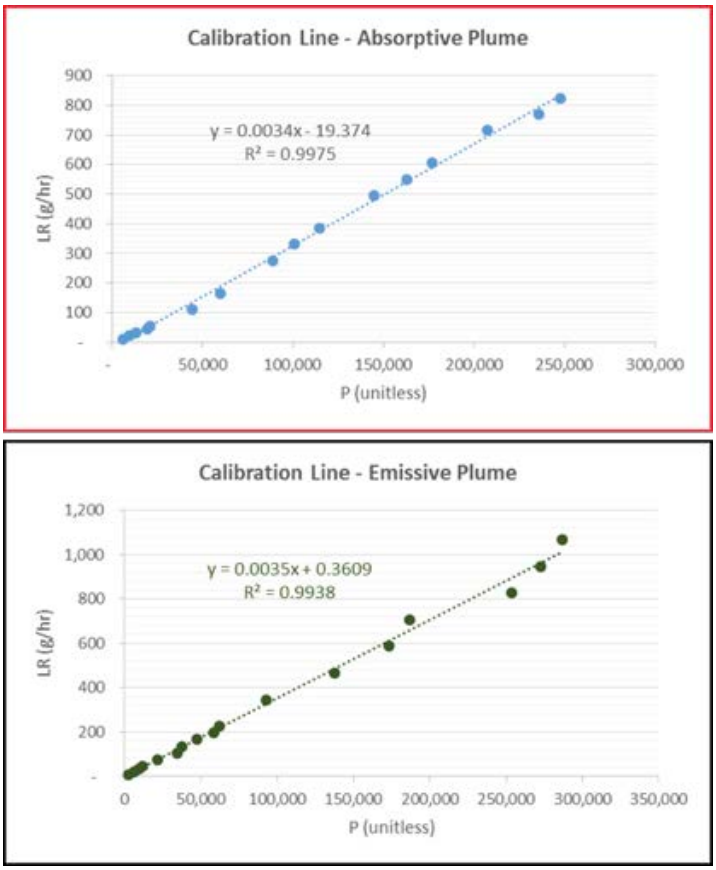

Figure 8: Sample calibration curves for QL-100 QOGI software.

Multiple approaches were proposed to establish a quantitative relationship between the pixel intensity difference with and without a plume (ΔI) and the product of concentration in ppm and path length in meters (ppm-m) for a gas column represented by a pixel in the IR image for a given temperature differential (ΔT) between ambient air and the background (Zeng, 2012). Eastern Research Group (ERG, 2014), under a contract with EPA, confirmed this quantitative relationship, showing that there is a monotonically increasing relationship between ΔI and concentration for a uniform black background that was temperature controlled. The ERG data also show that ΔI increases as the temperature of the background increases for a specific gas concentration.

The working principle of QOGI can be described as follows:

•IR images of a leak are analyzed for intensity on a pixel-by-pixel basis.

•Each pixel represents a column of hydrocarbon vapor between the camera and the background.

•Pixel contrast intensity (ΔI) is defined as the intensity difference at the pixel level between the background with and without the absorption due to hydrocarbon molecules.

•ΔI is a function of the temperature difference between the background and the plume (ΔT).

•At a given ΔT, the intensity is proportional to the number of hydrocarbon molecules in the vapor column.

•The leak rate is reflected in both pixel intensity and the number of pixels that have a ΔI higher than a certain threshold. Inversely, the combination of the two factors determines leak rate.

Based on the above referenced methodologies, a computer program (QL-100) has been developed that captures raw IR data from an IR camera and analyzes it for leak rate. The IR camera must be radiometrically calibrated to make it capable of measuring temperature at the pixel level. The calibration equation is LR = a P + b where LR is the leak rate (g/hr), P is the aggregated pixel intensity for the gas plume and a/b are constants. Calibration curves for QL-100 are shown in Figure 8. To analyze the IR images, the user must also input a measured ambient temperature and distance from the component being tested to the IR camera. The QL-100 program will then collect images for 30 seconds and use proprietary algorithms to automatically calculate the mass leak rate. All other variables required for determining leak rate are pre-programmed into the computer program. With the captured IR images and the two user- provided input parameters, the program will calculate the mass leak rate in grams per hour (g/hr) as seen in Figures 9 and 10.

Results

Field Testing & Qualification for the IntelliRed™ Technology

A prototype DIR imager was constructed using two cooled MWIR imagers with a common optical path. Each imager pro-

vides 640 x 512 pixels streaming video at 30 frames per second. A synchronized master clock provides temporal registration between the two imagers assuring good alignment for moving objects. The optic for the prototype DIR is a 25mm to 100mm F1.5 continuous zoom lens with motorized zoom and focus controls. Figure 11 shows a picture of the prototype imager.

Field testing the prototype DIR camera and algorithm demonstrated the ability to identify a hydrocarbon plume and distinguish it from common interferences such as people and steam. In the sample frame collected during field testing (Figure 12, p. 354), one can see the image from the gas band on the left and the reference band on the right.

Notice that the hydrocarbon plume appears as a dark shape in the gas band and is not present in the reference band. Both natural gas as a hydrocarbon mixture and propane as a pure hydrocarbon were used during these field tests. The white steam plume is present in both the gas band and reference band, though at a higher intensity in the gas band. The person appears in both the gas band and the reference band. Applying the techniques described above, the signal of the hydrocarbon plume is separated from the steam plume and other background objects. Figure 13 (p. 354) shows the resulting image with the hydrocarbon plume autonomously recognized and highlighted by colorizing the pixels red.

A significant benefit of these techniques is that the detection is accomplished in a single frame of video. This allows for a much simpler computer vision algorithm architecture that requires minimal processing power. The dual-sensor algorithm is compact enough that it could be deployed directly into the firmware of the IR camera, significantly reducing ancillary equipment requirements. Another benefit is that it allows leak detection to occur from a moving camera platform, lending itself to vehicle, marine or aerial based surveys. These results were repeated with multiple field tests utilizing various backgrounds and leak scenarios. The thresholds and techniques applied continue to develop with additional field testing improving the sensitivity and false alarm rejection rate.

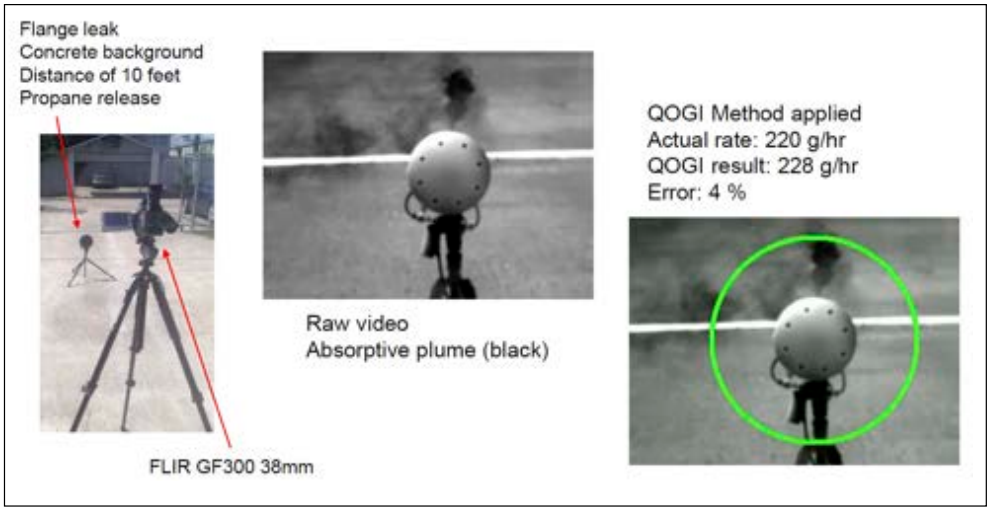

Figure 9: QOGI detection for a leak from a flange.

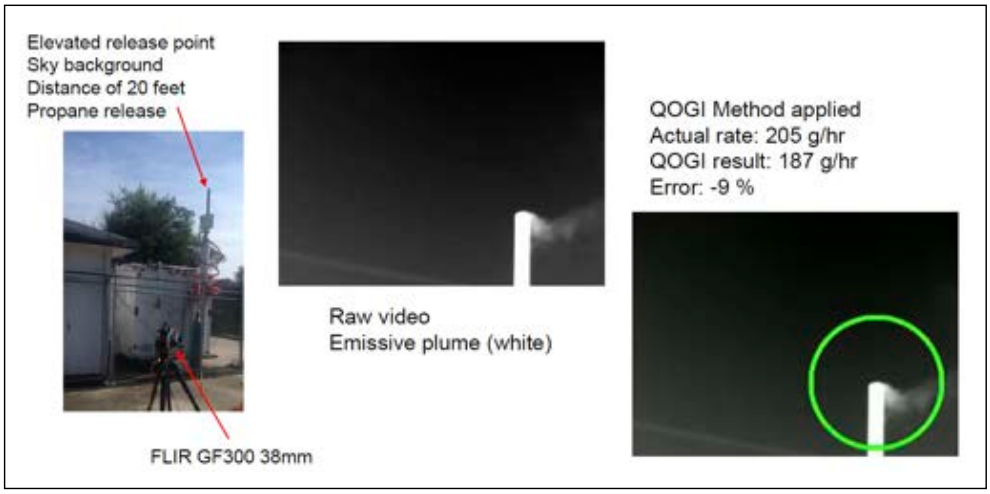

Figure 10: QOGI detection for a hydrocarbon plume released from a stack.

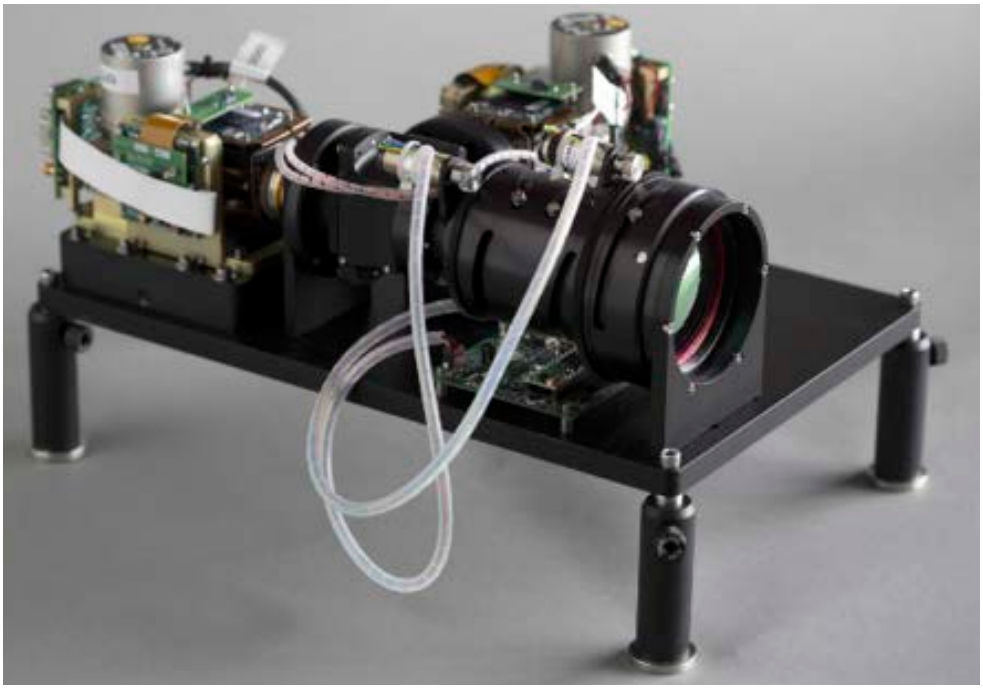

Figure 11: Prototype IntelliRed™ differential infrared system.

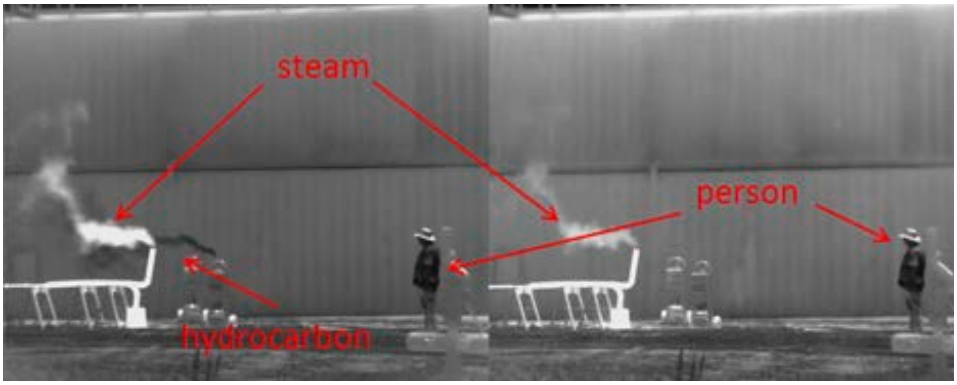

Figure 12: Spatially registered frame from gas band (left) and reference band (right) of differential infrared camera.

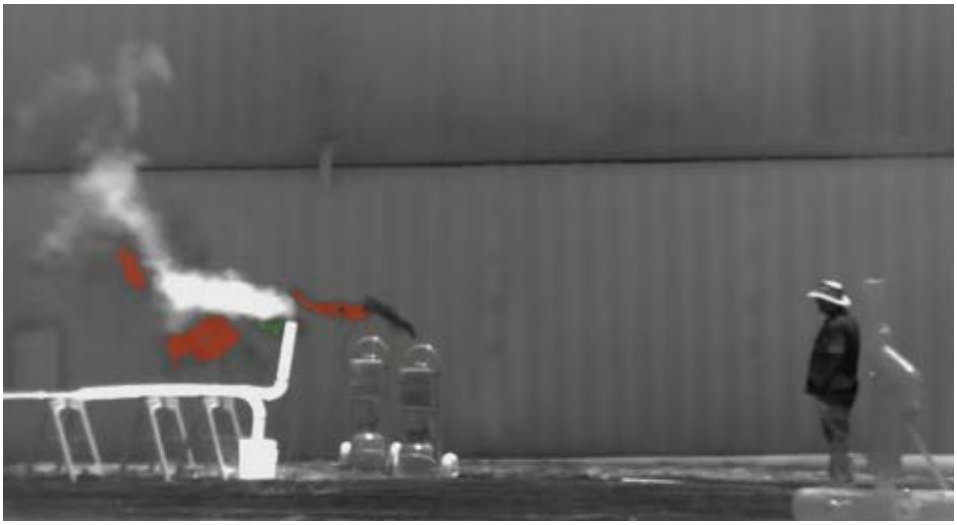

Figure 13: Resulting frame from the differential infrared algorithm.

Pilots & Commercial Deployments for the IntelliRed™ Technology

Deploying these IR imagers into industrial settings requires rugged camera enclosures to protect against the elements. Temperature, dust and humidity can all adversely affect the equipment's performance and lifetime. Figure 14 depicts a rugged enclosure developed for the deployment into an industrial setting.

This enclosure is sealed, pressurized and temperature controlled. Temperature control is provided with either thermoelectric cooling or instrument air. An integrated pressure switch monitors the pressure differential between the enclosure and ambient pressure and will disconnect power to the enclosure if the pressure differential drops below a set threshold.

In addition to the IR imager, a visible camera is co-located in the enclosure. All power systems, control signals and video streams are combined to a single mil-spec plug, providing a unified ethernet connection and single 48 V DC power supply. This allows the operator to control the camera assembly with a web-based interface utilizing ethernet protocols. This system has been deployed in Qatar since 2013 and similar systems have been deployed to facilities in Saudia Arabia and the U.S. Figure 15 shows the deployed system in Qatar (left) and the U.S. (right).

One significant challenge for the deployment in Qatar was keeping the enclosure interior temperature below the operating temperature for the imager and electronics. For deployments in the U.S., thermoelectrically cooled enclosures were sufficient to provide continuous operation. However, environmental testing showed that the thermoelectric coolers would not provide sufficient cooling for the harsh Qatar climate.

A new cooling system was designed to meet this challenge. A thermostatically controlled Vortex cooler uses high pressure (100 psi), high temperature (40 ºC or higher) instrument air to generate low pressure, low temperature air to cool the enclosure. While this introduces the need for instrument air at the deployment site, it provides a very robust cooling solution. Throughout the Qatar deployment, the system maintained operating temperature with a reliable instrument air supply. There were occasions when the air compressor supplying the instrument air failed. Figure 16 shows temperature data collected before and after a failure of the air compressor.

As the temperature data show, the enclosure is kept well within operating temperature limits with a supply of instrument air. When the instrument air supply failed, the interior temperature of the enclosure exceeded the operating temperature for the imager causing the system to shut itself off. Once the ambient temperatures dropped, the system was able to operate without instrument air and passive cooling only.

These field data show that the system can be operated continuously in the extreme climate of Qatar with a reliable instrument air supply. Another version of this enclosure has achieved ATEX EX II 1 G Exp IIA T3 (Zone 1) certification, enabling deployment in hazardous electrical environments. Based on the results of these deployments, a new sensor platform with a high-temperature imager has been developed that can achieve continuous operation in Qatar with passive

Figure 14: Rugged enclosure for IR optical gas imager

cooling only (no instrument air needed). Such systems will reduce deployment costs as the site preparations will be reduced to a single power supply and a single ethernet connection.

Comparing IntelliRed™ Technology & Existing Gas Detection Technologies

The most prevalent technologies used for leak detection are catalytic point combustible gas detectors, IR point detectors and IR path detectors. Catalytic point combustible gas detectors rely on the principle that when gas oxidizes it produces heat. The sensor generally includes two heating elements, with one element embedded in a catalyst. The surface of the catalyst reacts exothermically in the presence of hydrocarbons. This reaction generates heat, which changes the resistance of the embedded coil. The resistance of the embedded coil is measured via a standard Wheatstone Bridge-type circuit and compared to the reference coil. The change in resistance is proportional to the gas concentration.

One potential drawback of the catalytic combustible gas detectors is that the catalyst requires oxygen to operate. An oxygen deficient environment will reduce the efficiency of the oxidation and hence the sensor's accuracy. The catalyst can also be contaminated by dust, oil, grease and certain chemical compounds, such as silicones and sulfurs. This failure mode may not be easily detectable and so requires frequent calibrations of the sensor.

IR point combustible gas detectors have generally replaced traditional catalytic detectors for detecting lower explosion limit (LEL) hydrocarbon vapor measurement. The basic measurement principal of an IR point detector uses an IR source to illuminate a volume of gas that has diffused into a measurement chamber. If hydrocarbons are present in the measurement chamber, they will absorb certain wavelengths of IR energy as the light passes through the chamber while other wavelengths pass through completely unattenuated. Two optical sensors with different spectral sensitivity measure the change in intensity of the absorbed light compared to the non-absorbed light. This change in intensity is related to the concentration of the hydrocarbons in the measurement chamber.

Most commercially available IR point detectors can be calibrated for up to 100 target gases with a linearized 4-20 mA autosensing signal output corresponding to 0-100% full-scale deflection (FSD). That % FSD range, in turn, corresponds to 0 to 100% LEL with a certain degree of error (usually 1% to 2%). Each point detector has to be initially calibrated and then regularly tested with a 50% LEL canister of the target gas (most IR point detectors are initially calibrated with methane). Once an IR point detector is calibrated for a certain hydrocarbon (e.g., methane, propane), it can detect said gas even if it is released in a hydrocarbon mixture plume. The point IR detectors are sometimes deployed in pairs utilizing voting logic to reduce false alarms.

A potential issue with IR point detectors is insensitivity or signal drifting caused by water and water vapor in the measurement chamber (Baliga & Khan, 2016).

While IR point detectors rely on wind conditions to bring the hydrocarbon plume to the point detector, IR open path detectors can cover a wider area. The technology relies on an IR source and receiver, which are mounted at some distance from each other. The source and receiver are carefully aligned and calibrated to establish the response in the absence of a hydrocarbon plume. The distance between the source and receiver can be several hundred feet.

Figure 15: Deployed IntelliRed™ systems in Qatar (left) and the U.S. (right).

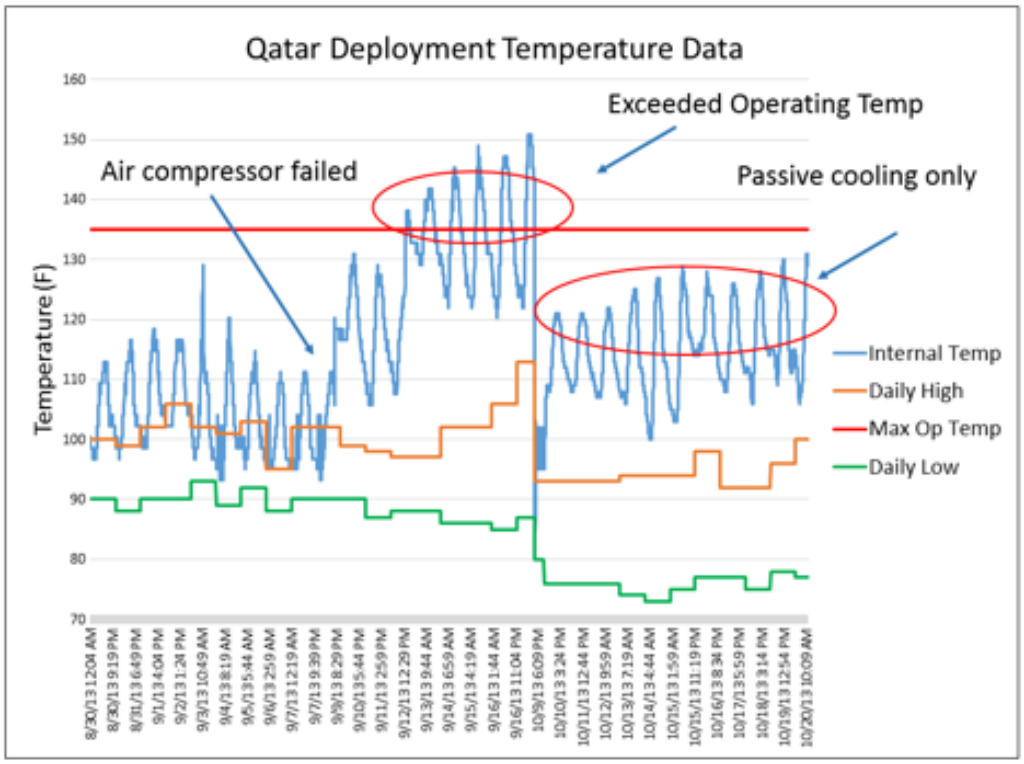

Figure 16: Temperature data for Qatar deployment site.

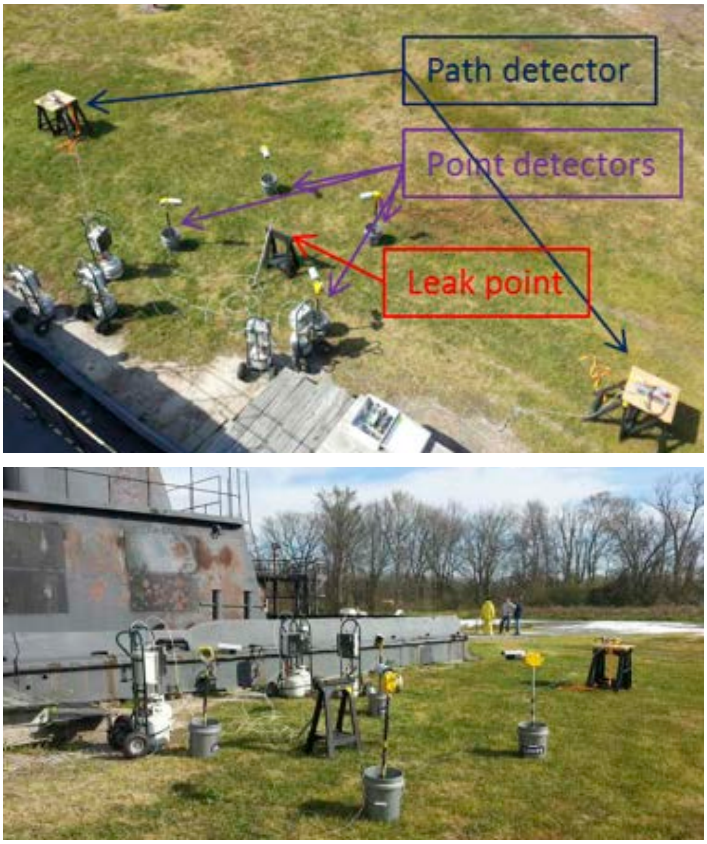

Figure 17: Field testing to compare IntelliRed™ system to point and path hydrocarbon detectors.

After calibration, the IR open path detector continuously monitors the signal from the source. If a hydrocarbon plume passes between the source and receiver, it will absorb certain wavelengths of IR energy. The receiver will detect the reduced energy level caused by the absorption of the hydrocarbon vapor. Due to the nature of open path measurement, the units of the detector are concentration by unit of distance, typically LEL-meters. Commercially available IR open path detectors are can be calibrated for up to seven target gases (methane, ethane, propane, butane, pentane, ethylene, propylene and butadiene) with a linearized 4-20 mA signal output corresponding to 0 to 5 LEL-m.

Leak Scenario	1	2	3	4	5	6	7	8	9	10	11
Leak Rate (l/min)	45	60	30	15	15	15	60	60	60	45	45
Point 1 Response (% LEL)	0.6	0	3.0	3.5	0	0	0	0	0	0	0
Point 2 Response (% LEL)	0	0	0	0	0	0	0	0	0	0	0
Point 3 Response (% LEL)	0	0.2	0	0	0	0	0	0.9	0	0	0.2
Point 4 Response (% LEL)	0	0	7.5	0	0	0	0	37.8	18	0	0
Path Response (LEL-m)	1.9	0	1.6	0.8	0	0	0	0.9	0	0	0

Table 2: IR point and path detector response.

IR open path detectors come in three open path ranges (short with a path length of 5-40m, medium with a path length of 40-120m and long with a path length of 120-200m). Most industrial IR open path detectors use multiple spectral filters to eliminate the interference from water vapor exhibited by IR point detectors. As a result, IR open path detectors can operate in high humidity conditions, including rain or fog. A potential issue for IR open path detectors is obstruction or misalignment of the IR source.

A series of field tests was conducted to compare the detection capability of the IntelliRed™ remote gas detection system to existing point and path IR technology. A representative sensor was selected for the two most common technologies (IR point detectors and IR open path detectors) based on a survey of the devices deployed at various facilities. Four IR point detector units were purchased and were calibrated to propane (0 to 100% LEL). Each unit has a response (T50—time to 50% of range) of 4.5 seconds. A short-range path detector (15 to 130 ft) with a measurement range from 0 to 5 LEL-m was chosen with a response time (T90—time to 90% of range) of 3 seconds. An alignment tool was also purchased to provide for calibration in the field.

The IntelliRed™ system was deployed with a 25mm to 100mm F1.5 continuous zoom lens. The zoom lens was set to the longest focal length (100mm) for each scenario. The algorithm thresholds and sensitivity settings were identical for each scenario, although three different backgrounds were selected. The IntelliRed™ algorithm was challenged with interferences (people) before each test to ensure that the sensitivity settings were reasonable for continuous deployment. The system was operated in autonomous mode during each leak scenario with no human interaction to facilitate detection. For the purposes of these field tests, the system was required to achieve three confirmations to successfully detect a leak.

In total, 11 field tests were conducted comparing the point and path detectors to the IntelliRed™ system. Propane gas was released at rates varying from 15 l/min to 60 l/min. The four point detectors were arranged in close proximity to the release point at a distance of 5 ft. The path detector was arranged to intersect with the plume at a point in close proximity to the release point. The IntelliRed™ system was positioned at distances ranging from 275 to 320 ft from the release point. Figure 17 shows images of a typical field test, with point detectors arranged in a diamond pattern around the release point and the path detector intersecting with the release point. The leak duration for each scenario was 10 minutes.

Prior to each field test, the point and path detector were calibrated. For the point detectors, a 50% LEL calibration gas was used to calibrate and then demonstrate the response of each detector. For the path detector, an alignment tool was utilized to ensure good signal and calibration performed using optical filters. The IntelliRed™ system successfully confirmed the leak in each of the 11 scenarios. The cumulative results from the point and path detectors are shown in Table 2.

The alarm levels for the IR point detectors are user defined, but common practice is to set the

alarm value at 50% LEL (approximate midpoint of the instrument range). With that threshold, none of the point detectors produced an alarm throughout the field testing. The highest reading from a point detector (37.8% LEL) was achieved during scenario 7 with a leak rate of 60 l/min at a distance of 5 ft from the leak source.

The open path detector alarm thresholds are also user defined. Common practice is to set the alarm value at approximately 50% of the detection range (or 2.5 LEL-m). With that threshold, the path detector did not alarm during any of the field tests. The highest response (1.9 LEL-m) was achieved during scenario 1 with a leak rate of 45 l/min and the path detector arranged to interact with the plume approximately 1 ft from the release point.

While these results are anecdotal, they show that the IntelliRed™ technology can remotely detect hydrocarbon leaks at levels that are well below the detection capability of existing technologies. IR point detectors are a mature technology and relatively inexpensive sensors, but they must come into contact with the hydrocarbon plume to achieve detection. In these field tests the point detectors were placed as close as 5 ft to the release point and rarely elicited a response from the small amount of propane released. In an actual deployment, the distance between the point detector and the leak source can be much greater as it is not practical to deploy point detectors every few feet. While the IR point detectors were placed in close proximity to the leak source, the IntelliRed™ system was positioned 300 ft away and achieved detection in each scenario.

IR point and path detectors also need to be calibrated to a specific target gas, which limits its application if a hydrocarbon release in near proximity does not include that specific component. The IntelliRed™ technology, with its MWIR-based sensors, does not need initial or ongoing calibration to a target gas since it is capable of detecting and visualizing multiple hydrocarbons in pure or mixture form at the same time (due to the superimposition of the carbon-hydrogen bond absorbance signal in the 3.3 to 3.5 µm range of the MWIR spectrum. Furthermore, IR point and path detectors cannot speciate the type of gas being detected, while LWIR based sensors could be easily integrated with the IntelliRed™ computer vision algorithm and possibly used for gas speciation with future hardware improvements.

The open path detector achieved more consistent results than the point detector, eliciting a response in four of the 11 scenarios. However, in each scenario the open path detector was positioned to intersect with the hydrocarbon plume 1 to 2 ft from the release point. As with the point detectors, in an actual deployment it will be rare that the path of an open path detector intersects with a leak within 2 ft of the source.

Field Testing & Qualification: Quantitative Optical Gas Imaging Technology

Work to date has measured component leak rates using the QOGI technology on accurately controlled releases, with the focus on propane. Two sets of field trials were set up by the research team in February 2015 and June 2015. Flow (or leak) rate was set using a calibrated Sierra SmartTrak 100 mass flow controller. The February 2015 dataset included 80 test runs with low leak rates while the June 2015 dataset included 111 test runs with high leak rates. In each of the two field tests, the IR camera was positioned 3 meters or 10 feet away from the release point. All of the tests performed to date were conducted in an outdoor, open air environment. The types of backgrounds tested included a uniform temperature controlled metal board, building wall, sky, concrete and gravel.

Leak rates ranged from 6 g/hr to 2,750 g/hr and site geometries included tubing, pipes and flanges. These tests included sunny and cloudy days, in sunlight and in shade, ambient temper-

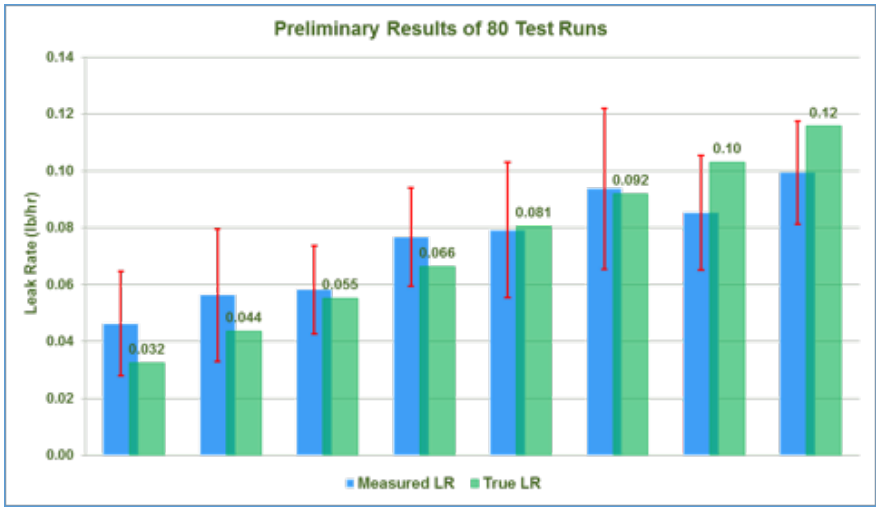

Figure 18.: Results of February 2015 QOGI field trials (80 tests conducted with propane).

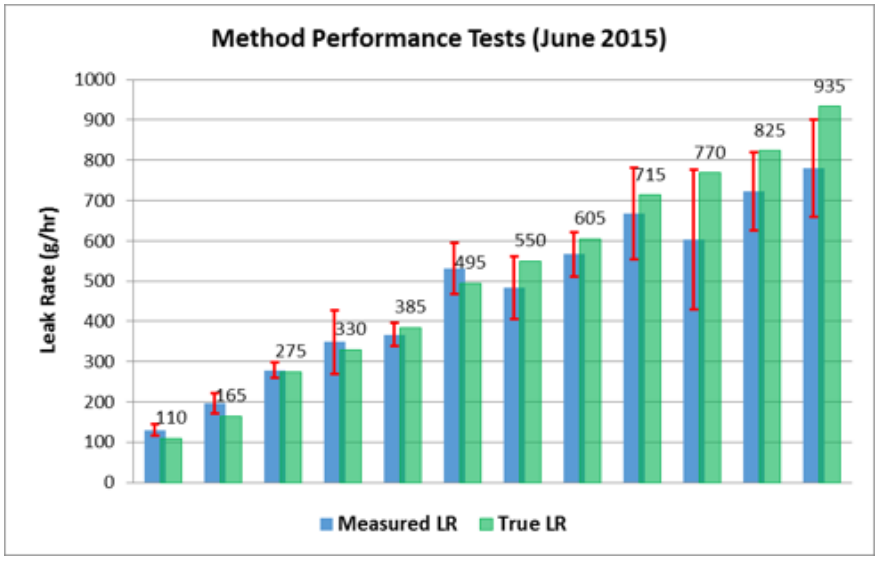

Figure 19: Results of June 2015 QOGI field trials (111 tests conducted with propane).

atures from 3 to 35 °C, relative humidity from 50% to 90%, and various moderate wind conditions up to 8 m/s. Because the true leak rates were known in these tests, the accuracy of this method can be assessed by comparing the true leak rate and the leak rate measured by QOGI as seen in the results presented in Figures 18 and 19 (p. 357). Within these two field trials, the measured leak rates were between -17% and +43% from the true values.

A limited number of tests were also performed for methane and ethylene. Leak rates were determined for these materials using IR response factors (RF) developed based on the IR spectra of methane and ethylene relative to the spectra of propane (PNNL). Measured leak rates used RFs developed from these known spectra (vs. direct measurement) and are summarized in Table 3.

Further testing of the QOGI technology was done at the EPA and Europe's CONCAWE Vito sites in 2015 and 2016. These tests included a mix of controlled leak scenarios (open pipe or LDAR leak cart, 26 releases of methane and propane, sky or complex background distances up to 16.5 m and leak rates from 70 to 4500 g/hr) and unknown leak rate scenarios (two toluene releases from a hot bucket at 40 m and one hydrocarbon release mixed with steam via a fog generator at 40 m). Data for the blind tests were collected on the spot and handed over to the regulators for review.

Detection error for these field tests ranged from -20% to +13%. These complex field trials were conducted to develop a quality assurance project plan (QAPP) that defines data quality indicators (DQI) for applying QOGI technology for quantification and to qualify IR based quantification methods by the regulators. These DQI will be relevant to regulatory approval of the QOGI technology as an alternative work practice under EPA regulations and other jurisdictions. EPA purchased the first commercially available QOGI product in 2016 to continue internal testing and performance evaluation.

Initial results for the qualification and performance evaluation of the QOGI technology are encouraging, especially when comparing measurement accuracy with the inherent uncertainties in Method 21. The uncertainties associated with Method 21 based methodology come from two potential sources:

•measured SVs;

•correlation equations that are applied to the SVs to estimate emissions rate.

The SV is a concentration measurement obtained by using a probe to "sniff" around a component to determine the maximum concentration. Concentration is not necessarily proportional to the leak rate, but is presumed to be for estimating leak rate using Method 21. Factors such as the geometry of the leaking component, the pressure inside the equipment, wind speed and atmospheric turbulence will affect the concentration measurement (or SV reading) and could introduce errors. Method 21 could yield significantly different estimates of leak rate for different leak scenarios, even when the leak rate is exactly the same.

Compound	Range of Leak Rates (lb/hr)	Number of Tests	Average Error %	Standard Deviation of Error %
Methane	0.12 to 0.24	25	24%	39%
Ethylene	0.03 to 0.11	20	19%	34%

Table 3: Initial results for methane and ethylene using QOGI.

The potential for error is also introduced when correlation equations are applied to the SV to estimate mass emission rate. The correlation equations were developed based on field tests in which SVs were determined using Method 21 and actual mass emissions rates were determined with another technique (usually through a bagging test) (EPA, 1995). The correlation between these paired data sets was not very strong, as indicated by low R^2 values from 0.32 to 0.54. Overall, errors in the leak rates estimated using the EPA protocol for Method 21 could be in the range of -100% to +400%, when all of the potential sources of error are propagated.

With Method 21, the concentration (not emission rate) is measured without regard to the totality of the leak plume, and the emission rates are estimated based on the concentrations and the empirical correlation equations. In comparison, QOGI treats the entire plume as an entity and directly measures mass leak rates (i.e., emission rates). For the range of tests reported in this paper, the errors in the QOGI results were substantially smaller than those that would be expected from application of Method 21.

Initial data have demonstrated the technically feasibility of measuring mass emission rates using an optical gas imaging device, which is currently a visual and qualitative tool. The initial data also indicate that QOGI technology has the potential to achieve better representativeness of emissions from individual leaking components than Method 21. QOGI directly measures emission rates. This is fundamentally different from Method 21, which estimates emission rates using screening values and correlation equations. With QOGI technology, operators only have to input ambient temperature and an approximate estimate of the distance from the leak site to the IR camera. QOGI technology can then capture the IR images for approximately 30 seconds and provide the operator with a measurement of the mass emission rate on the spot.

Integration of Quantification Features Into the IntelliRed™ Technology

Once the development of the QOGI technology was completed, the research effort switched to focusing on extending the capabilities of the IntelliRed™ technology to quantification of hydrocarbon plumes in addition to visual detection and confirmation. Lessons learned from the QOGI technology and the QL-100 software package were used to update the programming of the IntelliRed™ computer vision algorithm to allow it to autonomously quantify plumes at the pixel level and be analogous to a two dimensional array of open path detectors. The interface of the updated IntelliRed™ algorithm (Figure 20), shows concentration contours of the released gas in units of LEL-m (0-6 LEL-m range). Initial field testing and validation conducted in 2016 allowed for successful detection and quantification of methane and propane releases with further calibrations planned in the future.

Conclusions

IR optical gas imagers have proven to be an effective remote leak detection technology and are becoming widely used in recent years throughout the industry as handheld detectors. The IntelliRed™ autonomous detection system extends the capabilities of optical gas imagers enabling

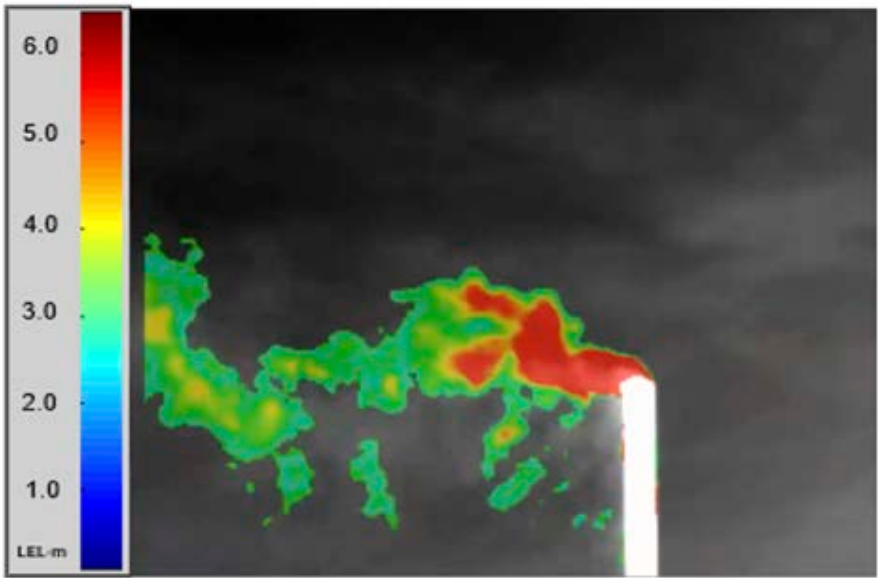

Figure 20: Quantification features in the IntelliRed™ technology.

autonomous remote leak detection and quantification. Combining this technology with rugged enclosures and advanced optics, it is possible for a single camera installation to cover a wide field of view providing continuous autonomous remote leak detection with detection limits that outperform existing technologies.

Existing IR point and open path detectors are quite effective at detecting large hydrocarbon clouds, but IntelliRed™ technology can also provide a means for early detection of much smaller leaks, reducing the potential of a higher consequence event. This technology is uniquely suited to monitor areas that are difficult to cover with existing technologies, such as elevated pipe racks or distillation columns. It can also provide a means to detect difficult leak scenarios, such as corrosion under insulation or periodic releases.

While existing IR point and open path detectors can alert an operator to the presence of hydrocarbons if the concentrations are high enough and wind conditions are favorable, IntelliRed™ technology provides an alert as well as a high contrast real time visual image to help the operator safely respond to the alarm. In addition, the ability to remotely stream the results of this system over an ethernet protocol provides the operator with a real-time tool to investigate leak alarms without putting personnel into harms way.

The advancement of a dual-sensor IntelliRed™ system opens up new applications. DIR is capable of generating an alarm in a single frame, providing immediate notice to the presence of a hydrocarbon plume. A frame-by-frame reference also provides very low false alarm rates, enabling applications where the system could be integrated into fire suppression systems. Single-frame alarming also opens up applications for detection from a moving platform. Aerial pipeline surveys with a dual-sensor system could be achieved, as well as surveys form vehicles and boats. The dual-sensor IntelliRed™ system is undergoing qualification with multiple pilot deployments underway. The commercially available dual-sensor system offers detection limits lower than the single-sensor systems with a lower false alarm rate.

In addition to process safety, the combined IntelliRed™ and QOGI technologies can extend the capabilities of LDAR programs and have the potential to reduce fugitive emissions and improve air quality (Zeng, Zhou, Katwala & Calhoun, 2006). In traditional LDAR programs, a FID or handheld IR optical gas imager is used to manually inspect components once per quarter. If the component begins leaking, it will go undetected between inspections. Using autonomous IntelliRed™ technology allows for increased monitoring frequency without the additional labor costs associated with traditional LDAR monitoring. Providing continuous monitoring allows a facility to quickly identify and correct large leak sources, which typically constitute 95% of fugitive emissions. ■

References

Baliga, S. & Khan, S. (2016). IR technology for fail-to-safe hydrocarbon gas detection. Retrieved from http://s7d9.scene7.com/is/content/minesafetyappliances/IR%20Gas%20Detection%20Technology%20White%20Paper

Benson, R., Madding, R., Lucier, R., et al. (2006). Standoff passive optical leak detection of volatile organic compounds using a cooled InSb- based IR imager (Paper 06-A-131-AWMA). In *Proceedings of the 99th Annual Meeting of the A&WMA, New Orleans, LA.*

EPA. (2014). Method 21: Determination of volatile organic compound leaks (Title 40, Part 60, Appendix A). Washington, DC: Author.

EPA. (1995). Protocol for equipment leak emission estimates (EPA-453/R-95-17). Washington, DC: Author.

EPA. (2008). Alternative work practice to detect leaks from equipment Retrieved from https://www.gpo.gov/fdsys/pkg/FR-2008-12-22/html/E8-30196.htm.

ERG, (2014, Jan. 14). Spectral testing of gas imaging cameras and spectral library (Work Assignment ETS-2-1). Washington, DC: EPA.

Pacific Northwest National Laboratory (PNNL). The PNNL quantitative IR database. Retrieved from https://secure2.pnl.gov/nsd/nsd.nsf/Welcome

Stein, S.E., Linstrom, P.J. & Mallard, W.G., (2013). IR spectra. In NIST Chemistry WebBook. Retrieved from http://webbook.nist.gov/chemistry

Zeng, Y. (2012). White paper on a calibration/verification device for gas imaging IR camera. Retrieved from http://providenceeng.tiltlabs.com/docs/White_Paper_-_IR_Camera_Calibration_or_Verification.pdf

Zeng, Y., Zhou, L., Katwala, N. & Calhoun, K. (2006). The third-generation LDAR (LDAR3): Lower fugitive emissions at a lower cost. Presentation at the National Petrochemical and Refiners Association 2006 Environmental Conference, San Antonio, TX.

A Markov Chain Approach to Domino Effects in Chemical Plants

Nima Khakzad, Mohsen Naderpour and Genserik Reniers

Abstract

We have introduced a methodology based on Markov chain for modeling domino effects in chemical plants. The graphical structure and modeling features offered by this chain make it possible to intuitively model the temporal and spatial escalation of domino effects. Accommodating conditional dependencies and complex interactions among the involved units, Markov chain can be used 1) to estimate the probability and duration of potential domino effects at different levels; 2) to identify the most probable sequence of events leading to a domino effect; and 3) to foresee whether a domino effect would terminate or escalate to the next level(s). The application of the methodology has been demonstrated via a hypothetical chemical storage plant.

Keywords

Domino effect; chemical plant; Markov chain; safety assessment

Chemical plants are normally characterized by atmospheric, cryogenic, and pressurized storage tanks, networks of pipelines, and production equipment containing, carrying, and processing hazardous materials usually in high-temperature high-pressure conditions. As a result, a normal incident (normal in terms of environmental or asset damages) or undesired event that could be tolerated or controlled in other industrial plants has the potential of turning into a catastrophe within a few hours due to the possibility of triggering domino effects (chain of incidents). Domino effects are high-impact low-probability (HILP) events in which a primary incident (e.g., fire) in a unit (e.g., storage tank) triggers secondary and higher-order events in neighboring units. The overall consequences of such a sequence of events are more severe than that of the primary incident (Reniers & Cozzani, 2013).

The propagation of the primary incident is usually facilitated by means of escalation vectors such as fire engulfment or heat radiation in the case of fire, and overpressure waves or projectile fragments in the case of explosions. These escalation vectors help propagate the primary incident by causing either loss of containment or loss of physical integrity of the secondary units. The probability of escalation, however, depends on a variety of factors such as the type and severity of escalation vectors, the distance between the primary and secondary units, the vulnerability of secondary units, and the type and inventory of chemical substances involved (Darbra, Palacios & Casal, 2010).

Although rare, domino effects are so severe in terms of human losses and environment damages that their inclusion in the risk analysis and safety assessment of chemical infrastructures seems indispensable. For instance, LPG–induced domino effects in Mexico City in November 1984 led to 650 deaths and 6,500 injuries, and destroyed three process plants. More recently, in December 2005, a vapor cloud explosion (VCE) and following fires in an oil storage plant in the Buncefield Complex, U.K., left 43 injured and destroyed homes and businesses. The fire started after an overflow of 250,000 liters of petrol from a storage tank (theguardian, 2012). A similar incident occurred at Caribbean Petroleum Refinery in 2009, where a VCE led to a series of fires (CSB, 2015).

The need for modeling and risk analysis of domino effects in chemical facilities has long been recognized (Bagster & Pitblado, 1991; Delvosalle, 1996; Gledhill & Lines, 1998; Khan & Abbasi, 1998; Reason, 1997), although the application of conventional probabilistic techniques has been limited owing to modeling complex interactions and dealing with low probabilities. The previous attempts at probabilistic modeling of domino effects include application of binomial distribution (Cozzani. Gubinelli, Antonioni, et al., 2005), game theory (Reniers, Dullaert & Karel. 2009), Monte Carlo simulation (Abdolhamidzadeh, Abbasi, Rashtchian, et al., 2010), Bayesian network (Khakzad, 2015; Khakzad, Khan, Amyott, et al., 2013), and event tree analysis (Landucci, Argenti, Tugnoli, et al., 2015; Landucci, Argenti, Spadoni, et al., 2016).

In the context of domino effects modeling, the probabilities of domino effects at sequential levels and the most probable escalation pattern of potential domino effects are of great interest especially to assign preventing and mitigating safety barriers as well as setting emergency firefighting action plans. The present work is aimed at examining the applicability of Markov chain (MC), which is intrinsically compatible with temporal and spatial evolution of stochastic events, to domino effect modeling.

The following sections present the fundamentals and relevant terminology of domino effects and MC; the methodology devel-

Nima Khakzad, Ph.D., PEng., is an assistant professor in safety and security science at Delft University of Technology (TU Delft), The Netherlands. He is also the co-chair of Chemical and Process Engineering Technical Committee at European Safety and Reliability Association. Khakzad can be reached at n.khakzadrostami@tudelft.nl.

Mohsen Naderpour, Ph.D., is a lecturer at the School of Systems, Management and Leadership in the Faculty of Engineering and Information Technology at the University of Technology Sydney (UTS). He is also a member of the Global Big Data Technologies Centre at UTS.

Genserik Reniers, Ph.D., is a professor in safety and security science at TU Delft. He is also a professor at Universities of Antwerp and KU Leuven, Belgium, and the co-chair of Occupational Safety Technical Committee at European Safety and Reliability Association.

oped; its application to a demonstrative case study; and the study conclusions.

Domino Effects

Domino effects take place when an incident in a unit (primary unit) propagates to other units (secondary units) by means of escalation vectors. Escalation vectors are physical effects such as fire impingement, fire engulfment or heat radiation in the case of a fire, and overpressure or projectile fragments in the case of an explosion. Methods for calculation of escalation vectors can be found in the TNO Yellow Book (1997), CCPS (2000), and Assael and Kakosimos (2010). The probability of escalation, however, depends not only on the type of escalation vectors but also on other factors such as the type and inventory of the chemicals involved, the separation distance between the primary and secondary units, and the vulnerability of the secondary units.

Further, to determine whether a secondary unit is likely to be affected by an escalation vector, the intensity of the escalation vector at the point of interest (i.e., the location of the secondary unit) should be higher than a corresponding threshold value. For example, for atmospheric vessels (e.g., atmospheric storage tanks) the threshold values for the heat radiation and the overpressure have been proposed as follows, respectively (Antonioni Spadoni, & Cozzani, 2009):

$$Q_{th} = 10\ \frac{kw}{m^2} \qquad P_{th} = 22\ kpa$$

Among methods available to estimate the escalation probabilities, probit models have been popular and widespread due to their simplicity and flexibility (Cozzani & Salzano, 2004; Cozzani, Gubinelli, Antonioni, et al., 2005; Cozzani, Gubinelli & Salzano, 2006; Landucci, Gubinelli, Antonioni, 2009). Using probit models for process equipment, usually both the type of equipment and the type of escalation vector the equipment receives are taken into consideration to calculate a probit value Y in the form of:

$$Y=a+b\ \ln(D) \qquad (1)$$

where a and b represent probit coefficients determined using experimental data and regression methods; D is either the escalation vector (e.g., heat radiation intensity) or relevant parameters such as time to failure ttf of secondary equipment or the peak static overpressure Ps.

Table 1 (p. 366) presents some probit models used in the literature for atmospheric and pressurized equipment exposed to heat radiation and overpressure (Cozzani, et al., 2005).

Markov Chain

MC is a probabilistic tool to model stochastic processes that develop over time. One common form of MC is the homogeneous discrete-state continuous-time MC in which the system under consideration is assumed to be in one of n discrete states and the transition rate ρ_{ij} from state S_i to state S_j not only depends on the current state of the system S_i but also remains constant over time. Assuming constant transition rates among the states implies exponential probability distributions for time in a MC (Ramakumar, 1993).

Having the transition rates, the transition probability from S_i to S_j in a small time interval Δt is $p_{ij}= \rho_{ij}\Delta t$. Thus, according to the law of total probability, the probability of being in S_i at $t+\Delta t$, i.e. $P_i(t + \Delta t)$, will be the probability of being in S_i at time t and remaining in the same state (which equals the unity minus the probability of leaving the same state) during Δt plus the probability of being in other states than S_i at time t and transitioning to S_i during Δt:

$$P_i(t+\Delta t) = P_i(t)\left(1 - \sum_{j=1,j\neq i}^{n} \rho_{ij}\Delta t\right) + \sum_{j=1,j\neq i}^{n} P_j(t)\rho_{ji}\Delta t \qquad (4)$$

Rearranging and dividing Equation (4) by Δt, Equation (5) is obtained as $\Delta t \to 0$:

$$\frac{dP_i(t)}{dt} = \sum_{j=1,j\neq i}^{n} P_j(t)\rho_{ji} - P_i(t) \sum_{j=1,j\neq i}^{n} \rho_{ij} \qquad (5)$$

Solving Equation (5) for all states along with the additional equation:

$$\sum_{i=1}^{n} P_i(t) = 1$$

the time-dependent probabilities of the system's states can be calculated under appropriate initial conditions. Developing the MC of a stochastic system, some other useful information can also be derived about the system under consideration. For example, the expected time the system will remain in S_i that is denoted by τ_i τcan be represented as the reciprocal of the summation of the transition rates from S_i to other states (Ramakumar, 1993):

$$\tau_i = \frac{1}{\sum_{\substack{j=1 \\ j\neq i}}^{n} \rho_{ij}} \qquad (6)$$

Markovian Approach to Domino Effect

Model Development

Consider a simple example where a process plant consists of only two storage tanks, T1 and T2, containing flammable chemical liquids. Assuming negligible explosivity of the contained chemicals, three modes can be envisaged for each tank, that is: Safe (S), on Fire (F) and Burned out (B). As such, the entire plant would end up with at most $3^2 = 9$ states denoted by S1 to S9 (Figure 1, p. 367). For example, S6 in Figure 1 represents the state in which both T1 and T2 are on fire, whereas S8 denotes the state where T1 is still on fire while T2 has already burned out due to the complete combustion of the contained flammable liquid.

Transition Rates

After identification of the system states, the possibility of transition between the states of the system should be examined. Transition from S_i to S_j should be in complete conformance with the principles of domino effect escalation and characteristics of the states. In this regard, various factors such as type and intensity of escalation vectors, possibility of synergistic effects, type

and extent of ongoing incidents in each state, type and amount of involved chemicals, ttf and time to burn out ttb of storage tanks, and particularly the temporal sequence of accidents in a domino effect should be taken into consideration.

To make the discussion more concrete, consider the transition from S1 to S2 in Figure 1. Comparing S2 with S1, the only difference is the change in the mode of T1 from safe (S) to on-fire (F). Thus, the corresponding transition rate (in this context, the failure refers to a loss of containment of T1 followed by an ignition, causing T1 to catch fire) would be equal to the failure rate of T1 due to operational or environmental factors rather than domino effect escalation vectors, which can be estimated using historical data or conventional risk analysis methods such as fault tree and event tree. The individual failure rates of T1 and T2 have been denoted as λ_i in Figure 1.

Being in S2, the system, however, can transition to either S4 or S6, depending on whether the heat radiation (escalation vector) emitted from T1, which is on fire in S2, is high enough (greater than Q_{th}=10 kw/m^2) to cause a credible damage to T2. If so, S2 would transition to S6, escalating the domino effect to the first level; otherwise, the fire in T1 would burn out without affecting T2 and, thus, S2 transitions to S4.

In the former (i.e., transition from S2 to S6), the transition rate would be equal to the failure rate of T2 due to the heat radiation emitted from T1, denoted by ρ_{12}. Since for very small time intervals the failure rate can be defined as the ratio of the failure probability to time (Ebeling, 1997), ρ_{12} can be estimated as the ratio of the failure probability of T2 to the ttfof T2.

In the latter (i.e., transition from S2 to S4), the transition rate, however, would be equal to the burn-out rate of T2, denoted by μ_1, due to the complete combustion of the contained chemicals. Assuming a constant burn-out rate, μ_1 can be estimated as the reciprocal of the mean value of ttb which, in turn, depends on both the burning rate and inventory of the chemicals contained in T2. Methods to calculate burning rates of liquids and gasses can be found in Assael and Kakosimos (2010).

As shown in Figure 1, in state S4, T1 has been burned out while T2 is still in the safe mode. Thus, it is yet likely that the mode of T2 changes from safe to on fire, making the system transition from S4 to S7. Since this transition is not due to a domino-effect-induced escalation vector (T1 is not on fire; thus the failure of T2 is not due to T1), the corresponding transition rate would be equal to the individual failure rate of T2. This transition rate has been denoted in Figure 1 by λ_2. It is worth noting that since the transition from S4 to S7 (and from S5 to S8 alike) has not been provoked by an escalation vector, it is not taken into account in the modeling of domino effect; this is why the respective arrow in Figure 1 has been drawn with dashed line. As a result, S4, S5 and S9 would be considered as terminal states in which the domino effect ceases to exist or develop.

Markov Chain Analysis

Using the MC developed in Figure 1, the time-dependent probabilities of all the states can be calculated by simultaneously solving the set of ordinary differential equations given by Equation (5) and an extra equation:

$$\sum_{i=1}^{6} P_i(t) = 1$$

This equation is subject to appropriate initial conditions. The most common initial condition is the assumption of the system being in S1 at t = 0, that is $P_1(0) = 1$ and $P_{(i\neq1)}(0) = 0$.

The time-dependent probability of the zero-level domino effect, in which the primary event has not yet escalated to other units, can be calculated as $P_{(Domino\text{-}0)}(t) = P_2(t)+P_3(t)$.

Further, by using Equation (6) the duration of the zero-level domino effect would be equal to the average residence time in S2 and S3; that is:

$$T_{Domino-0} = \frac{\lambda_1}{\lambda_1+\lambda_2}.\frac{1}{\mu_1+\rho_{12}} + \frac{\lambda_2}{\lambda_1+\lambda_2}.\frac{1}{\mu_2+\rho_{21}}$$

In the foregoing relationship,

$$\frac{\lambda_1}{\lambda_1+\lambda_2} \text{ and } \frac{\lambda_2}{\lambda_1+\lambda_2}$$

refer to the conditional probabilities of being in S2 and S3 at t + Δt, respectively, given that the system was in S1 at t.

During a domino effect, it is also possible to predict the termination of, or the escalation of the domino effect to the next level. For example, if the system is in S2 (zero-level domino effect), the probability of transition to S4 (termination of the primary accident without triggering a domino effect) after a time interval Δt would be:

$$P\left(S_4^{t+\Delta t}\middle|S_2^t\right) = \frac{\mu_1}{\mu_1+\rho_{12}}$$

while the probability of transition to S6 (escalation of the primary accident to the first-level domino effect) would be:

$$P\left(S_6^{t+\Delta t}\middle|S_2^t\right) = \frac{\rho_{12}}{\mu_1+\rho_{12}}$$

Likewise, the probability of the first-level domino effect can be estimated as:

$$P_{Domino-1}(t) = P_6(t) + P_7(t) + P_8(t)$$

while its duration would be equal to the summation of the residence time in S6 and average residence time in S7 and S8 as:

$$T_{Domino-1} = \frac{1}{\mu_1+\mu_2} + \frac{\mu_1}{\mu_1+\mu_2}.\frac{1}{\mu_2} + \frac{\mu_2}{\mu_1+\mu_2}.\frac{1}{\mu_1}$$

In this case:

$$\frac{\mu_1}{\mu_1+\mu_2} \text{ and } \frac{\mu_2}{\mu_1+\mu_2}$$

are the conditional probabilities of being in S7 and S8 at t + Δt, respectively, given that the system were in S6 at t.

Using the developed MC, it is also possible to estimate the likelihood of the temporal sequence of events in a domino effect. Not to mention that such sequences should not only be physi-

cally possible but also should not contradict with the escalation mechanism of the domino effect. As a result, the most probable sequence (MPS) of events or alternatively the most probable escalation pattern of the domino effect can be identified. This will help allocate appropriate preventing or mitigating safety measures to prevent from the initiation or escalation of a potential domino effect. The probability of a potential sequence of events such as S1 -> S2 -> S6 -> S8 can thus be estimated as:

$$P(S1, S2, S6, S8) = P(S1)\, P(S2|S1)\, P(S6|S2)\, P(S8|S6) = e^{-(\lambda_1+\lambda_2)t} \cdot \frac{\lambda_1}{\lambda_1+\lambda_2} \cdot \frac{\rho_{12}}{\mu_1+\rho_{12}} \cdot \frac{\mu_2}{\mu_1+\mu_2}$$

Application of the Methodology

Case Study

For the sake of clarity, the application of the methodology is exemplified using a demonstrative chemical storage plant including three atmospheric storage tanks T1, T2, and T3 (Figure 2, p. 367). The characteristics of the tanks are reported in Table 2 (p. 366). Because of the illustrative purposes, pool fire and heat radiation are considered as the only accident scenario and escalation vector, respectively. Besides, T1 is chosen as the primary unit where a domino effect can initiate.

Transition Rate Calculation

The corresponding MC has been depicted in Figure 3 (p. 368). Assuming a wind speed of 2 m/s from the southeast measured at 10 m above the ground, air temperature of 20 ºC, relative humidity of 50%, a partly cloudy sky, stability class of F and a circular opening diameter of 15 cm for leakage, the burning rate and pool fire diameter of T1 are calculated as 820 kg/min and 18.9 m, respectively. Likewise, the burning rate and pool fire diameter of T2 and T3 are calculated as 863 kg/min and 15.1 m. The heat radiation intensity received by Tj from Ti is reported in Table 3 (p. 366).

Aside from the individual failure rates (transition rates from S1 to S2, S3 and to S4 in Figure 3), which have been assumed identical for all the tanks as $\lambda = 2.19$ E-10min^{-1}, the required burn-out rate μ and domino-induced failure rates ρ_{ij} can be estimated using the burning rates and heat radiation intensities (Table 3).

For example, the transition rate from S2 to S5 which would be equal to the burn-out rate of T1, $\mu 1$, can be estimated as the reciprocal of the mean value of ttb of the entire content of acetone contained in T1. According to the mean burning rate, 820 kg/min, and a mass of 400 ton of acetone in T1, the mean ttb of T1 would be estimated as 487.8 min. Thus, $\mu 1 = 1/487.8 = 2.05$ E-03 min^{-1}. Likewise, the burn-out rates of T2 and T3 would be estimated as $\mu 2 = 7.19$ E-03 min^{-1} and $\mu 3 = 1.08$ E-02 min^{-1}.

Similarly, the transition rate from S2 to S8 can be estimated as the failure rate of T2 due to the heat radiation from T1. Inserting the quantities of $Q_{12} = 16.2$ kW/m^2 (Table 3) and $V_2 = 200$ m^3 (Table 2) in the probit model of atmospheric equipment (Table 1), the corresponding ttf and probit value of T2 are calculated as ttf= 852 s (or 14.2 min) and Y = 0.0772, respectively.

Substituting Y in Equation (2) or (3), the failure probability of T2 would be calculated as 4.27 E-05. Dividing the failure probability by ttf, the domino-induced failure rate of T2 (or equivalently the transition rate from S2 to S8) would be estimated as:

$$\rho_{12} = \frac{4.27\text{ E}-05}{14.2} = \ 3.0\text{ E-06}$$

Following the same procedure, the transition rate from S8 to S17 can be calculated as the failure rate of T3 due to the synergistic effect of T1 and T2, in which the heat radiation received by T3 is the summation of heat radiations emitted from both T1 and T2.

Thus, the value of heat radiation needed to be used in the probit model is:

$$Q_{12-3} = Q_{13} + Q_{23} = 9.35 + 21.1 = 30.45\ \text{kW/m}^2$$

As a result, the respective transition rate would be $\rho_{(12\text{-}3)} = 2.24$ E-03. It is also worth noting that since the heat radiation intensity T3 receives from T1 is below the threshold value (i.e., $Q_{13} = 9.35 < Q_{th} = 10$), the failure rate of T3 due to T1 would be negligible, that is $\rho_{13} = 0$. As a result, there would not be any transition from S2 to S9 or from S12 to S22; this has been denoted by dashed arrows in Figure 3. Likewise, the other transition rates can be calculated.

Likelihood Modeling

Using the MC developed in Figure 3 and the calculated transition rates, characteristics such as time-dependent probabilities of the domino effect at different levels, the probability of termination or escalation to next levels, and probabilities of temporal and spatial sequences of events can be identified. For example, the time-dependent probabilities of the zero-level, first-level, and second-level domino effects can be estimated as:

$$P_{\text{Domino}-0} = P_2(t) + P_3(t) + P_4(t)$$

$$P_{\text{Domino}-1} = P_8(t) + P_9(t) + P_{10}(t)$$

$$P_{\text{Domino}-2} = P_{17}(t) + P_{21}(t) + P_{22}(t) + P_{23}(t)$$

These probabilities have been depicted in Figure 4 (p. 369) for a 24-hour time interval (1,440 minutes).

Further, given that the system is in state S3 (a zero-level domino effect), the probability of the domino effect termination will be:

$$P(S6 \mid S3) = \frac{\mu_2}{\mu_2 + \rho_{21} + \rho_{23}} = 0.983$$

Accordingly, the probability of the escalation to the first level will be:

$$P(S10 \mid S3) = \frac{\rho_{21}}{\mu_2 + \rho_{21} + \rho_{23}} + \frac{\rho_{23}}{\mu_2 + \rho_{21} + \rho_{23}} = 0.017$$

Also, given that the domino effect is in the first level (i.e., the system has started from S3 and is currently in S8 or S10), the probability of escalation to the second level will be:

$$P(S8 \mid S3)\,P(S17 \mid S8) + P(S8 \mid S3)\,P(S11 \mid S8)\,P(S21 \mid S11) + P(S10 \mid S3).P(S17 \mid S10) + P(S10 \mid S3).P(S15 \mid S10).P(S23 \mid S15) + P(S10 \mid S3).P(S16 \mid S10).P(S22 \mid S16)$$
$$= \frac{\rho_{21}}{\mu_2+\rho_{21}+\rho_{23}}.\frac{\rho_{12-3}}{\mu_1+\mu_{2+}\rho_{12-3}} + \frac{\rho_{21}}{\mu_2+\rho_{21}+\rho_{23}}.\frac{\mu_1}{\mu_1+\mu_2+\rho_{12-3}}.\frac{\rho_{23}}{\mu_2+\rho_{23}} + \frac{\rho_{23}}{\mu_2+\rho_{21}+\rho_{23}}.\frac{\rho_{23-1}}{\mu_2+\mu_3+\rho_{23-1}} + \frac{\rho_{23}}{\mu_2+\rho_{21}+\rho_{23}}.\frac{\mu_3}{\mu_2+\mu_3+\rho_{23-1}}.\frac{\rho_{21}}{\mu_2+\rho_{21}} + \frac{\rho_{23}}{\mu_2+\rho_{21}+\rho_{23}}.\frac{\mu_2}{\mu_2+\mu_3+\rho_{23-1}}.\frac{\rho_{31}}{\mu_3+\rho_{31}} = 3.75\ \mathrm{E}-03$$

As noted, one meritorious modeling technique offered by MC is the possibility of deriving the probability of any temporal sequence of (physically possible) events in a domino effect. For example, assume we are interested in knowing the probability of a sequence of events, given that the system is initially in S1, such as: (T2 catches fire -> the fire escalates to T3 -> T2 is burned out -> the fire escalates to T1 -> T3 is burned out -> T1 is burned out). This sequence of events corresponds to transition of the system as S1 -> S3 -> S10 -> S16 -> S22 -> S26 -> S27. Accordingly, the respective probability can readily be estimated as the joint probability distribution:

$$P(S1, S3, S10, S16, S22, S26, S27)$$
$$= P(S1)\,P(S3 \mid S1)\,P(S10 \mid S3)\,P(S16 \mid S10)\,P(S22 \mid S16)\,P(S26 \mid S16)\,P(S27 \mid S26)$$
$$= \frac{\lambda_2}{\lambda_1+\lambda_2+\lambda_3}.\frac{\rho_{23}}{\rho_{23}+\mu_2+\rho_{21}}.\frac{\mu_2}{\mu_2+\mu_3+\rho_{231}}.\frac{\rho_{31}}{\rho_{31}+\mu_3}.\frac{\mu_3}{\mu_1+\mu_3} = 1.021\ \mathrm{E}-08$$

It should be noted that in the foregoing joint probability distribution, P(S1) =1.0 since it is assumed that the system has initially been in S1. In a similar way, the most probable sequence (MPS) of events can be identified. For example, the MPS leading to a second-level domino effect such as S1 -> S3 -> S8 -> S17 which is equivalent to the sequence of events as: (T2 catches fire -> fire escalates to T1 -> fire escalates to T3). The corresponding probability is calculated as 5.61 E-04.

It is worth noting that the concept of MPS introduced in this study is slightly different than the most probable explanation (MPE) of events offered by Bayesian network (Khakzad, et al., 2011). In MPE, the most probable configuration of events contributing to an accident is determined regardless of the time line according to which the events take place. However, using MPS, the temporal order of the events takes precedence over their combinatorial probability (usually product of probabilities). In other words, according to MPS, for example, a sequence of three events with respective probabilities of $0.8 \times 0.2 \times 0.1$ is given priority over another sequence with respective probabilities of $0.2 \times 0.85 \times 0.1$. This is why the sequence S1 -> S3 -> S8 -> S17 is identified as the MPS despite the fact that S1 -> S3 -> S10 -> S17 results in a greater combinatorial probability $0.333 \times 0.00801 \times 0.2521 = 6.72$ E-04.

Knowing the MPS, not only the most probable escalation pattern (both temporal and spatial) of the potential domino effect can be identified, but also the most vulnerable units (storage tanks in this study) contributing to the escalation of the domino effect can be specified. As a result, appropriate preventing or mitigating safety measures can be allocated to these vulnerable units in order to eliminate or reduce the escalation probability of the domino effect. These safety measures can be either in the form of separation distances between the vulnerable units when the construction of a chemical facility is still in the design stage or in the form of threshold inventories in the vulnerable units in the case of existing facilities. In the former case, i.e., application of safety distances, transition rates of type ρ_{ij} would be reduced whereas in the latter case, i.e., application of safety inventories, transition rates of type μ_i would be increased (fire will burn out faster before finding a chance to escalate) by decreasing the chemical inventories of vulnerable units.

Discussion

In the present study, we demonstrated an application of MC to spatial and temporal modeling of domino effects in chemical plants. Chemical plants are complex systems normally attributed to nonlinearity, interlinked dependencies, and dynamic behavior. As a result, an incident that can readily be tolerated or controlled in other industrial facilities can potentially lead to a domino effect. The dynamic nature of domino effect itself which stems from its temporal and spatial escalation mechanisms further complicates the modeling of domino effects. MC has been proved to be a versatile tool in domino effect modeling where not only the identification of contributing units but also their sequential entrainment in the domino effect matters when predicting the likelihood of termination or escalation to next levels.

Aside from the meritorious modeling features of MC, there are drawbacks that hinder its widespread application to large chemical plants, where the developed MC can become cumbersome and error-prone. This is due to the notorious state-space explosion problem of MC in which the number of states and thus differential equations grow exponentially with the size of the chemical plant. For example, as shown in Figure 3, the number of states for the small plant presented in Figure 2 can count to 27 states. Adding another storage tank to the plant, the number of states could have risen to 81 states (three times as large as the former case).

Similarly, considering other possible accident scenarios such as vapor cloud explosion (VCE) or fire protection systems in place such as sprinkler and water deluge systems can further add to the number of states, thus making the developed MC even more cumbersome and time consuming. For example, if storage tank T2 in Figure 2 were equipped with a sprinkler system to suppress the fire, T2 in the MC of Figure 3 would include another state, namely "suppressed."

Accordingly, the transition rate from "burning" state to "suppressed" state, γ, could have been determined based on the efficacy and performance of the sprinkler system. Alternatively, the effect of the sprinkler system could have been taken into account by adding the transition rate to the "burn-out" transition rate (i.e., $\mu + \gamma$), without the need for adding the state "suppressed" to the model. Although there are techniques such as state merging to reduce the number of states, these techniques can only been applied under specific circumstances such as symmetrical Markov

models with identical transitional rates which are barely the case in real domino effects. A recent application of dynamic Bayesian network to risk assessment of domino effects in the presence of fire protection systems can be found in Khakzad, Landucci and Reniers (2017).

In this study we assumed a homogenous MC where the transition rates remain constant over time. For example, since S26 takes place after S2 according to the domino effect time-line depicted in Figure 3, it is likely that respective environmental and operational conditions such as wind speed and thus burning rates as well as heat radiation intensities for these two states would not be exactly the same. As a result, the transition rate from S2 to S5 with that of S26 to S27, which are considered the same as μ_1, would not be identical.

Likewise, the transition rates from S2 to S5 and from S8 to S11 which are presumably taken identical as μ_1 would not be the same; this is because in state S8, compared to S2 in which only T1 is on fire, both T1 and T2 are on fire. Thus, the burning rate of T1 would be accelerated due to the additional heat radiation received from T2. In other words, if the transition rate from S2 to S5 could be represented by μ_1, the transition rate from S8 to S11 would be equal to μ_{1^+}, where $\mu_{1^+} \geq \mu_1$.

Conclusions

In this study, we examined the applicability of Markov chain for domino effect modeling in chemical facilities. We illustrated how the continuous-time framework of Markov chain can be used to portray the temporal and spatial escalation of domino effects. Accordingly, the probabilities of any (physically possible) sequence of events, likelihood of termination or escalation at arbitrary time instances, and duration of domino effect in each level can be estimated. As a result, the most probable sequence of events during a potential domino effect can be identified. This latter achievement is worthwhile since in a dynamic process such as domino effects not only the combination of events but also their sequential entrainment in the chain of incidents matters.

Knowing the most likely sequence of events, a more effective allocation of preventing and mitigating safety barriers can be carried out to prevent or control the escalation of domino effects. The present study does not aim to replace available techniques such as Bayesian network but rather it is an attempt to provide more insight into the probabilistic modeling of domino effects as a dynamic phenomenon. ■

References

Abdolhamidzadeh, B., Abbasi, T., Rashtchian, D., et al. (2010). A new method for assessing domino effect in chemical process industry. *Journal of Hazardous Materials, 182,* 416-426.

Antonioni, G., Spadoni, G. & Cozzani, V. (2009) Application of domino effect quantitative risk assessment to an extended industrial area. *Journal of Loss Prevention in the Process Industries, 22,* 614-624.

Assael, M.J. & Kakosimos, K.E. (2010) *Fires, explosions and toxicgas dispersions: Effects calculation and risk analysis*. Boca Raton, FL: CRC Press, Taylor and Francis Group.

Bagster, D.F. & Pitblado, R.M. (1991). The estimation of domino incident frequencies: An approach. *Process Safety and Environmental Protection, 69,* 195-199.

Boudali, H. & Dugan, J.B. (2005). A discrete-time Bayesian network reliability modeling and analysis framework. *Reliability Engineering and System Safety, 87,* 337-349.

CCPS. (2000). *Guidelines for chemical process quantitative risk Analysis* (2nd ed.). New York, NY: AIChE.

Chemical Safety and Hazard Investigation Board (CSB). (2010). Caribbean Petroleum tank terminal explosion and multiple tank fires (Report No. 2010.02.I.PR). Retrieved from http://www.csb.gov/caribbean-petroleum-refining-tank-explosion-and-fire

Cozzani, V. & Salzano, E. (2004). The quantitative assessment of domino effects caused by overpressure: Part 1—Probit Models. *Journal of Hazardous Materials, A107,* 67-80.

Cozzani, V., Gubinelli, G., Antonioni, G., et al. (2005). The assessment of risk caused by domino effect in quantitative area risk analysis. *Journal of Hazardous Materials, A127,* 14-30.

Cozzani, V., Gubinelli, G. & Salzano, E. (2006). Escalation thresholds in the assessment of domino accidental events. *Journal of Hazardous Materials, 129,* 1-21.

Darbra, R.M., Palacios, A. & Casal, J. (2010). Domino effect in chemical accidents: Main features and accident sequences. *Journal of Hazardous Materials, 183,* 565-573.

Delvosalle, C. (1996). Domino effects phenomena: definition overview and classification. In *Proceedings of the European Seminar on Domino Effects, Leuven, Belgium.*

Ebeling, C.E. (1997). *An introduction to reliability and maintainability engineering* (2nd ed). New York, NY: McGraw Hill.

Gledhill, J. & Lines, I. (1998). Development of methods to assess the significance of domino effects from major hazard sites (CR Report 183). Sudbury, U.K.: Health and Safety Executive.

Khan, F. & Abbasi, S.A. (1998). Models for domino analysis in chemical process industries. *Process Safety Progress, 17,* 107-123.

Khakzad, N., Khan, F. & Amyotte, P. (2011). Safety analysis in process facilities: Comparison of fault tree and Bayesian network approaches. *Reliability Engineering and System Safety, 96,* 925-932.

Khakzad, N., Khan, F., Amyotte, P., et al. (2013). Domino effect analysis using Bayesian networks. *Risk Analysis, 33*(2), 292-306.

Khakzad, N. (2015). Application of dynamic Bayesian network to risk analysis of domino effects in chemical infrastructures. *Reliability Engineering and System Safety, 138,* 263-272.

Khakzad, N., Landucci, G., Reniers, G. (2017). Application of dynamic Bayesian network to performance assessment of fire protection systems during domino effects. *Reliability Engineering and System Safety, 167,* 232-247.

Landucci, G., Gubinelli, G., Antonioni, G., et al. (2009). The assessment of the damage probability of storage tanks in domino events. *Accident Analysis and Prevention, 41,* 1206-1215.

Landucci, G., Argenti, F., Tugnoli, A., et al. (2015). Quantitative assessment of safety barrier performance in the prevention of domino scenarios triggered by fire. *Reliability Engineering and System Safety, 143,* 30-43.

Landucci, G., Argenti, F., Spadoni, G., et al. (2016). Domino effect frequency assessment: The role of safety barriers. *Journal of Loss Prevention in the Process Industries, 44,* 706-717.

Neapolitan, R. (2003). *Learning Bayesian networks.* Upper Saddle River, NJ: Prentice Hall.

Ramakumar, R. (1993). *Engineering reliability: Fundamentals and applications.* Upper Saddle River, NJ:Prentice Hall.

Reniers, G. & Cozzani, V. (2013). Domino effects in the process industries. Amsterdam, Netherlands: Elsevier.

Reniers, G., Dullaert, W. & Karel, S. (2009). Domino effects within a chemical cluster: A game-theoretical modeling approach by using Nash-equilibrium. *Journal of Hazardous Materials, 167,* 289-293.

The Guardian. (2010). Buncefield fire: Oil storage firm found guilty of safety breaches. Retrieved from http://www.theguardian.com/uk/2010/jun/18/buncefield-fire-oil-company-guilty

EPA. (2007). ALOHA user manual. Retrieved from http://bit.ly/2iqSoWO.

Van Den Bosh, C.J.H. & Weterings, R.A.M.P. (1997). Methods for the calculation of physical effects (Yellow Book). The Hague, Netherlands: Committee for the Prevention of Disasters.

Type of equipment	Escalation vector	Probit model
Atmospheric	Heat radiation	$Y = 12.54 - 1.847 \ln(ttf)$
		$\ln(ttf) = -1.13 \ln(Q) - 2.67\times10^{-5} V + 9.9$
Atmospheric	Overpressure	$Y = -18.96 + 2.44 \ln(Ps)$
Pressurized	Heat radiation	$Y = 12.54 - 1.847 \ln(ttf)$
		$\ln(ttf) = -0.95 \ln(Q) + 8.85 V^{0.032}$
Pressurized	Overpressure	$Y = -42.44 + 4.33 \ln(Ps)$

Having Y determined, the escalation probability could be estimated as:

$$Pr = \phi\,(Y - 5) \quad (2)$$

where ϕ is the cumulative density function of the standard normal distribution. For spreadsheet applications, however, the escalation probability can alternatively be approximated from the following relationship:

$$Pr = 50\left\{1 + \frac{Y-5}{|Y-5|}\,\boldsymbol{erf}\left(\frac{|Y-5|}{\sqrt{2}}\right)\right\} \quad (3)$$

where erf is the error function.

Table 1: Probit models for heat radiation (Cozzani, et al., 2005).

Vessel	Type	Chemical	Volume (m^3)	Inventory (ton)
T1	Atmospheric	Acetone	500	400
T2	Atmospheric	Benzene	200	120
T3	Atmospheric	Benzene	200	80

Table 2: Chemical storage plant characteristics.

Ti↓ Tj→	T1	T2	T3
T1	-	16.2	9.35
T2	21.1	-	21.1
T3	12.7	21.1	-

Table 3: Heat radiation intensity (kW/m^2) received by Tj from Ti.

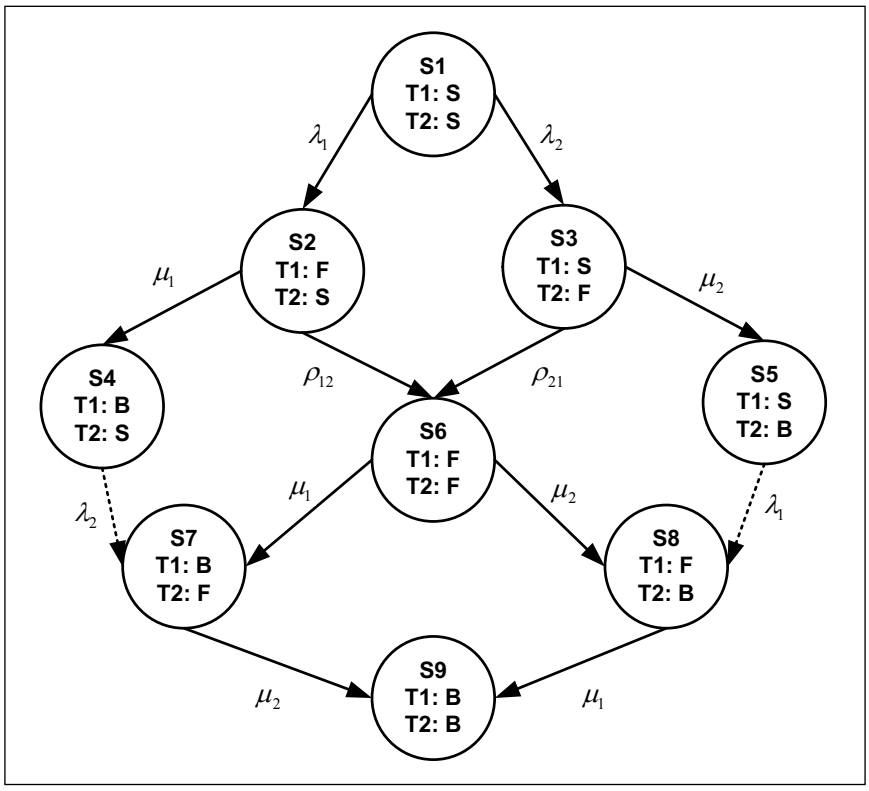

Figure 1. Markov chain for a domino effect in a chemical plant comprising two storage tanks T1 and T2. A dashed arrow from S4 to S7 (and from S5 to S8) implies that the corresponding transition is not accounted for in the domino effect modeling since this transition is not the result of an escalation vector.

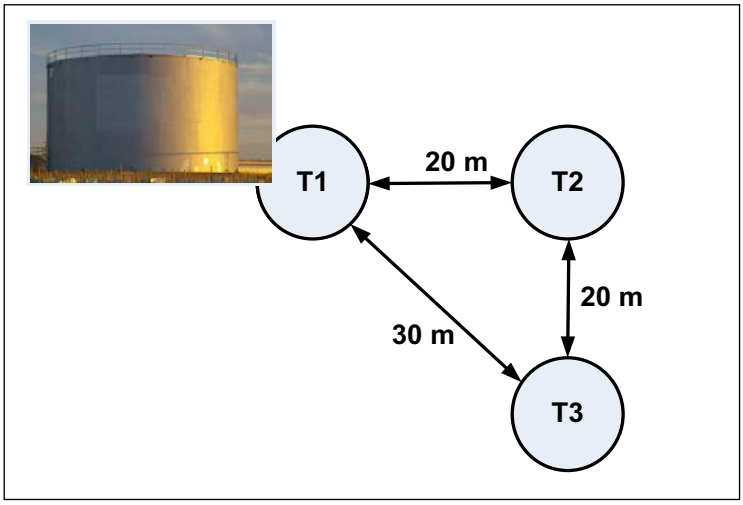

Figure 2: Schematic of process plant including three atmospheric chemical storage tanks.

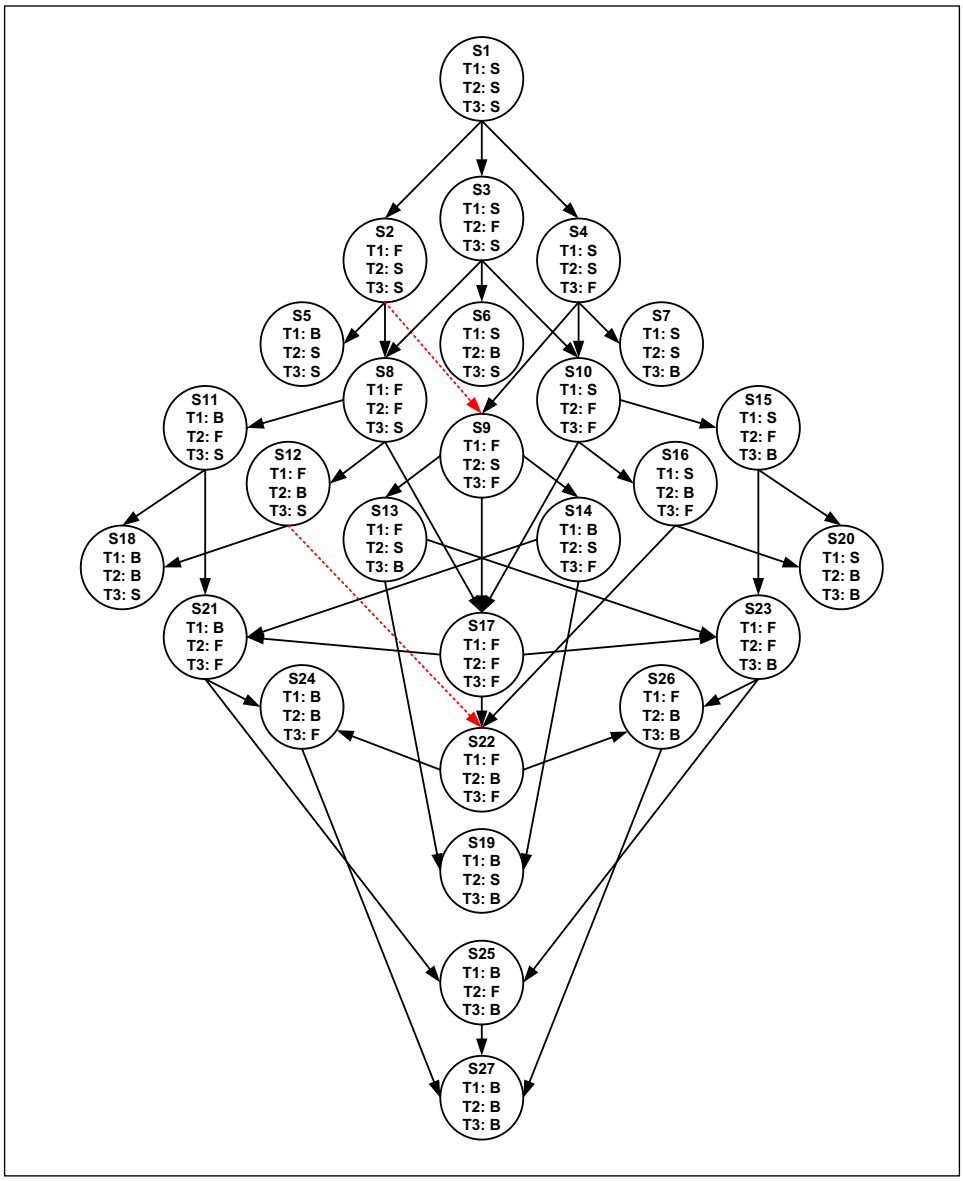

Figure 3: Markov chain for a domino effect in the chemical storage plant presented in Figure 2.

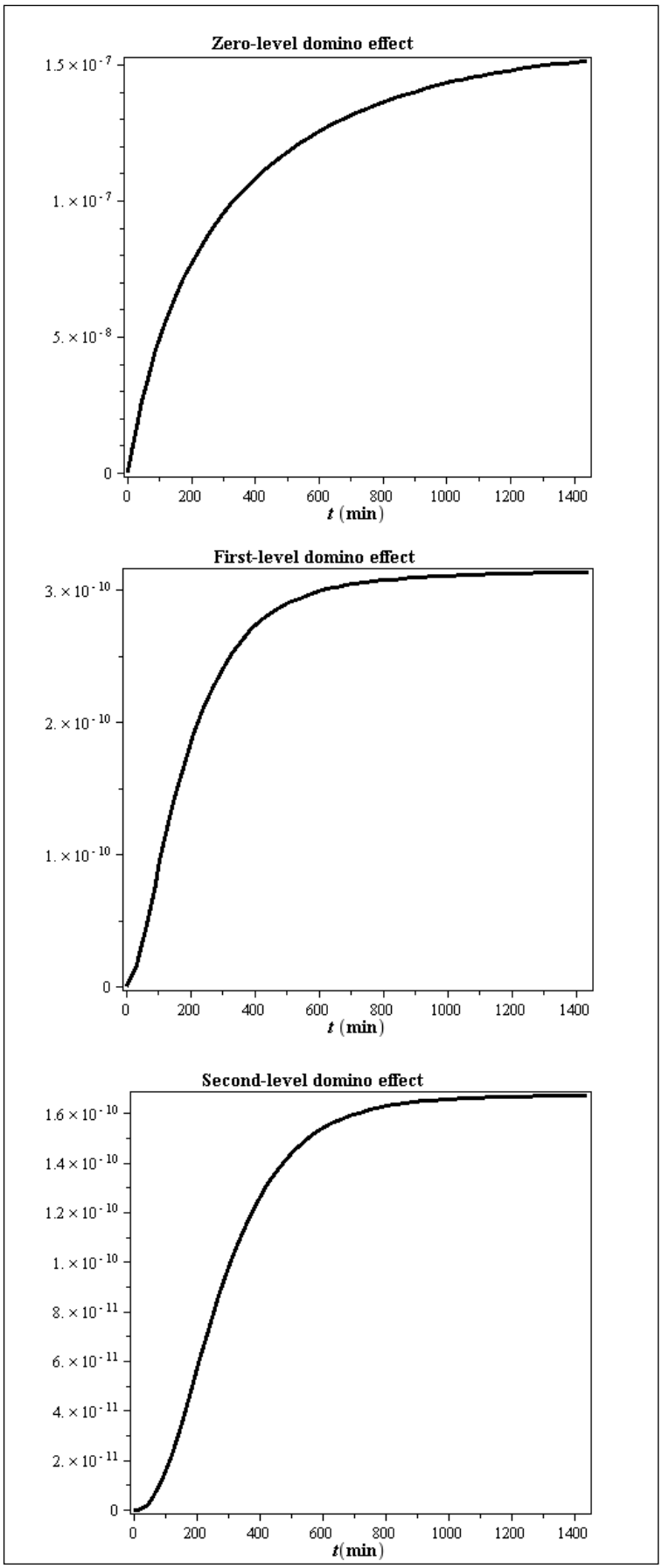

Figure 4: Time-dependent probabilities of the zero-level (A), first-level (B) and second-level (C) domino effects for 1,440 minutes (24 hours).

Impact of Design Completeness, Clarity & Stability on Construction Safety

Matthew Hallowell, Anthony Veltri, Christofer Harper, John Wanberg and Sathy Rajendran

Abstract

This article has made the first attempt to explore the empirical relationship between various characteristics of project design and safety performance. Specifically, design completeness and clarity was indicated by the frequency and magnitude of formal requests for information (RFI); design stability during construction was represented by the rate and magnitude of change orders (CO); and safety performance was represented as the rate of first aid and recordable injuries. Because there is a dearth of robust data relating indicators of design and safety performance, a mixed-methods research approach was employed.

First, data were collected from 20 design-bid-build projects to uncover if an empirical relationship exists among the variables. Second, interviews were conducted with the project managers of the 18 projects to explain why any observed relationships exist. The results indicate that, as the magnitude and frequency of COs and RFIs increase, the recordable injury rate increases. Interviews revealed that there is a perception among contractors that a clear, complete, and stable design facilitates a more predictable and, thus, safer construction environment. The implications of these findings is that there may also be inherent characteristics of a project design that affect safety performance. These results may encourage practitioners to ensure clarity in design that minimizes disruption and reduces the need for change orders to promote safety and constructability.

Keywords

Safety; design fidelity and clarity; labor and personnel issues

For the last decade, the U.S. construction industry accounted for more fatalities than any other industry [Bureau of Labor Statistics (BLS), 2016]. In fact, construction fatality rates are almost three-times the average rate among all industries. Although construction fatality rates have declined significantly in the last century, injury rates have plateaued (BLS, 2016). Researchers and practitioners remain perturbed by this phenomenon and seek new knowledge that enables more effective injury and fatality prevention efforts.

To establish new knowledge that will improve construction worker safety performance, researchers have conducted studies that evaluate new and existing construction safety management strategies, including those implemented by owners, contractors, designers, and subcontractors (Rajendran, 2006). Safety innovations may be mandated, facilitated, or implemented by these project players at various stages of a project lifecycle including the conceptual (Hinze, 1997; Szymberksi, 1997); design (Behm, 2005; Hinze & Gambatese, 1996), and construction phases (Esmaeili & Hallowell, 2012). Among these project phases, the concept of prevention through design (PTD) has gained great popularity in the academic community with over 100 peer-reviewed papers in the last 10 years.

Early articles on PTD in construction included theory that the ability to improve worker safety is greatest in the conceptual and design phase of a project (Syzmberski, 1997). Although this theory has only been tenuously supported through empirical data, a large volume of research has been conducted to better understand the theoretical benefits of PTD. Much of this research focuses attention on the theoretical benefits of PTD (Christensen, 2011), attitudes toward PTD (Toole & Marquis, 2004), legal implications (Gambatese, 1998), and methods and tools to enable PTD (Gambatese, 2004). The general epistemological position of the research community has been that specific design decisions can improve specific construction activities. For example, designing a parapet wall that is high enough to be in compliance for fall

Dr. Matthew Hallowell is a President's Teaching Scholar and Endowed Professor of Construction Engineering at the University of Colorado at Boulder. Dr. Hallowell specializes in construction safety research and education.

Dr. Anthony Veltri is an Associate Professor of Environment, Safety & Health at Oregon State University. Dr. Veltri does research on topics such as economic analysis of environment, safety and health issues and practices.

Dr. Christofer Harper is an assistant professor and holder of the McCollister Family Professorship in the Bert S. Turner Department of Construction Management at Louisiana State University. Dr. Harper's primary areas of research include project delivery, relational contracting, project management and administration, safety, decision support systems, emerging technologies and alternative energy.

Dr. John Wanberg is the Knowledge Strategy Manager at Stantec, a 22,000 person firm providing full lifecycle design and construction services. Dr. Wanberg received is PhD from the University of Colorado at Boulder in Construction Engineering and Management. His primary research areas were in organizational issues and governance of multinational construction and engineering organizations.

Dr. Sathy Rajendran is an Associate professor and Program Director of the Safety and Health Management Program within the Engineering Technologies, Safety, and Construction Department at Central Washington University. His research focus on construction safety management and education.

protection, would protect workers from falls during construction and maintenance (Gambatese, 2004). These design solutions offer compelling and often elegant safety solutions that, if implemented, would likely improve overall performance.

Despite these theoretical advancements, researchers have yet to explore potential connection between more general and innate characteristics of design and safety performance. For example, the following questions remain:

1) Does the clarity and completeness of design prior to construction relate to safety performance?

2) Does the stability of design during construction relate to safety performance?

The present article attempts to answer these questions. Here, design completeness is defined as the extent to which the design documents convey all of the necessary information needed for a competent contractor to build the final product. Design clarity is defined as the extent to which the design documents are easy for a contractor to understand and interpret. Finally, design stability is defined as the extent to which the design documents change during construction. Although there are variety of forces that affect these variables and are beyond the designer's control (e.g., the need to fast-track a project, the competency of the contractor, and unforeseen conditions), these variables are all inherently tied to design.

When measuring these variables, we posit that design clarity and completeness are indicated by the frequency and magnitude of the contractor's formal requests for information (RFIs). RFIs are formal documents with legal implications where the contractor requests design clarifications from the designer when building a project. Similarly, we posit that design stability is indicated by the frequency and magnitude of change orders (COs). According to Article 7.2.1 of American Institute of Architects (AIA, 2007) A201 document:

> a change order is a written instrument prepared by the Architect and signed by the Owner, Contractors and Architect stating their agreement upon all of the following: (1) the change in the work, (2) the amount of the adjustment, if any, in the contract sum, and (3) the extent of the adjustment, if any, in the contract time. (p. 27)

Although not perfect indicators, RFIs and COs are often tracked on projects because they are legally-binding documents. As such, they may provide valuable insight to the inherent characteristics of the design and their relationship to safety performance can be studied for the first time.

Understanding the impact of design completeness, clarity, and stability will help practitioners to better evaluate the potential safety implications of design. In addition to evaluating specific design elements (e.g., skylights, parapet walls), designers may wish to also evaluate the clarity of the design documents and the extent to which contractors will be able to perceive and interpret the desired meaning. Facility owners and designers should think carefully about potential implications of design changes once construction is under way. In addition to being expensive, they may cause instability in the construction process and, indirectly, injuries.

It should be noted that this study focuses on the design-bid-build project delivery method. In these project arrangements, the design is typically completed, bids are solicited and awarded, and construction typically begins with complete design documents. Other project delivery methods like design-build are vastly different in nature because of the inherent collaboration between the design team and the construction team, who may often be employed by the same organization or joint venture. Design-bid-build remains the predominant project delivery method in most construction sectors.

Literature Review

To establish a theoretical point of departure, literature related to prevention through design and the impact of COs and RFIs on project performance were reviewed. Literature and authors' experience were used as a guidance in the formation of the operational definitions. To date, there has yet to be a study that directly relates RFIs or COs to safety performance, although these constructs have often been implicitly discussed in the context of constructability reviews. When researchers discuss the feasibility of design (i.e., constructability), the potential implications for safety are often noted as a reason for such reviews. Similarly, we adopt the position that a more thorough check of design documents may be associated with improved safety performance. In addition to reviewing whether the design is "buildable," reviewing the clarity and completeness of the design may also be of economic value. This article builds upon general theory of prevention through design and constructability but departs by exploring the safety implications of previously unstudied constructs.

Prevention Through Design

In many ways, PTD is a form of safety constructability review, where the safety implications of design decisions are evaluated and alternatives are considered. PTD generally refers to the consideration of the safety of construction workers during the design phase of a project to eliminate or avoid hazards before any exposure occurs (Gambatese, et al., 2005). PTD can exist in many forms, ranging from formal team reviews and the use of tools to a more integrated approach where safety is intended to be considered in each design decision (Toole & Gambatese, 2008).

PTD researchers have made great strides in understanding how designs can be altered to prevent injuries (Behm, 2005), the implications of public policy (Gambatese, et al., 1997), perceptions of designers and clients (Behm & Culvenor, 2011), and theoretical benefits of implementation (Gambatese et al., 2005). The epistemological position of most researchers is that specific design decisions can make specific work environments safer to build. Although the authors do not refute this position, we broaden the perspective to note that indicators related to design such as clarity, completeness, and stability may also affect safety in more general, subtle and indirect ways. Additionally, we posit that these factors may not be controlled completely by designers and may be more related to project organization, communication, incentives and strategy.

Relationships Between RFIs & COs & Project Performance

RFIs and COs are common, legally binding forms of project documentation that occur between the design team who typically act as the facility owner's agent and the construction team. RFIs

are submitted to owner/designer team by the construction team to clarify elements of the design that are unclear as a facility is being built. Because the responses to these questions may have cost and quality implications, they are submitted in writing and responses are signed. Typically, all parties on a project keep detailed records of RFIs and the associated responses for legal reasons. Unlike RFIs, which are initiated by the construction team, a CO is work that is added, deleted, or modified from the original scope of work that is initiated by the owner/designer. COs are provided by the owner/designer to the construction team in writing, often with a request for budget and time modification that is subsequently accepted or negotiated. Like RFIs, COs are legally binding records and are retained by all parties.

RFIs and COs are interesting constructs in that they may be symptoms of the project type and scope, organization of the project team, competency of the project team, incentives structure, and even the economy. They may also be drivers of performance if they cause disruption or uncertainty for the construction team. Thus, they may be mediating variables that do not indicate any one type of behavior or project characteristic. This may explain why, despite the fact that RFIs and COs are easily accessed empirical data, there is relatively little research on how they relate to overall project performance.

Here, we consider RFIs to be an indicator of design clarity and completeness. Regardless of their ultimate cause, RFIs are submitted when something in the design is missing or unclear (Hanna, et al., 2012). The RFI may also be submitted when a contractor is not competent enough to understand a design that is complete and clear. In either case, the RFI is an indicator of a lack of understanding of the design (Mohammed, et al., 1999). Similarly, COs are made by the owner/architect but they may be ultimately caused by a variety of circumstances ranging from an error in design to changing preferences of the owner (Stocks & Singh, 1999). Again, regardless of their ultimate cause, they represent change to the design during construction that may disrupt the construction process to varying degrees.

Although researchers have explored the relationship between COs and project outcomes, the relationship between RFIs and project outcomes has been studied to a lesser extent. Interestingly, RFIs have been studied as they relate to project communication, knowledge dissemination, project team efficiency, and virtual teaming (Hanna, et al., 2012). RFIs have been considered as an indicator of efficiency and, often, as a process that is a candidate for improvement through the use of technology and enhanced collaboration tools. However, the ultimate impact of RFIs on project outcomes, including safety, has not been studied. This may result from the legal sensitivity of the documentation, the lack of definition of RFIs as a robust indicator of specific project characteristics, the variability in content and importance of RFIs, or the lack of understanding of the root causes of RFIs.

The research connecting COs to project performance is more robust, related, in part, to a better understanding of the causes of COs. For example, researchers have identified the following underlying causes:

•field conditions that are not reflected on the contract drawings (Stocks & Singh, 1999);

•client dissatisfaction with the design once construction begins (Stocks & Singh, 1999);

•building/design code changes that occur after a contractor award; (Stocks & Singh, 1999);

•poor site survey and site planning (Wu, et al., 2005);

•delays of owner supplied access or equipment and, discrepancies between the original design specifications, and contract documents (Perkins, 2007);

•design errors and omissions, and unforeseen conditions (Clarke, 1990).

Many research studies have concluded that construction COs decrease project performance (Alnuaimi, et al., 2010; Hanna, et al., 1999a; Hanna, et al., 2002; Ibbs, 1997). Researchers have also studied the general impact of change on performance, even in cases where a formal CO is not issued. Thomas & Napolitan (1995) examined the impact of construction changes on labor productivity. Based on an analysis of daily productivity values from three industry projects, they found that the average effect of all construction changes was a 30% loss of labor efficiency. They found a strong relationship between the rates of changes, disruptions, and rework. The most significant disruptions are the lack of materials and information and having to perform work out-of-sequence. Examples of disruptions include lack of materials, lack of tools or equipment, congestion and incidents. Hanna, et al. (1999a, b) supported these findings. Further, Kaming, et al. (1997) studied design changes associated with 31 high-rise projects in Indonesia and found that design change was the most important factor causing delays.

Although studies have not shown a direct relationship between COs and safety performance, impacts of COs may theoretically have an indirect impact on safety performance because of delays and resulting schedule pressure and impacts to worker morale. Rajendran (2006) collected opinion-based data from a 15-member Delphi safety expert panel and found that trade stacking, schedule compression, and less-qualified labor can lead to reduced safety performance. Furthermore, Gambatese et al. (2007), based on the results from a single project pilot study, reported that site congestion can have a negative impact on worker safety performance. Anecdotal evidence indicates when projects face cost and time overruns contractors tend to indirectly compromise safety.

Because an increase in the rate of COs decreases worker morale, and increases trade stacking, congestion, and schedule compression (Hanna, et al. 1999a, b), we believe that there may be a connection between the rate of COs and safety performance. It is here that we build on and deviate from the current body of knowledge.

Hypotheses & Research Question

Following directly from the relationships found in the literature, we formed testable null hypotheses:

H1) There is no correlation between the frequency and magnitude of change orders and construction safety performance.

H2) There is no correlation between the number of worker-hours needed to address change orders and construction safety performance.

H3) There is correlation between the rate of requests for information and construction safety performance.

If the null hypotheses are false, the resulting research question becomes: Why is there a relationship between design fidelity and construction safety performance? To answer this question we aimed to obtain observational data from the project managers. Such data supplement the findings and provide clear reasons for the statistical inferences.

Contributions to Theory & Practice

We make two chief contributions to theory in this study. First, we attempt to study the aforementioned hypotheses for the first time using empirical data and attempt to explain any relationships using qualitative data from interviews. Such research may elucidate the relationship between RFIs and COs on safety performance. Second, via interviews, we also explore the extent to which incidents are related to design clarity, completeness, and stability, using RFIs and COs as indicators. Although not direct indicators (e.g., RFIs may be caused by a contractor's lack of understanding rather than a deficiency in the design), we contribute to the knowledge base by exploring the connection or the first time.

We offer a new position that the general characteristics of the design, independent of any one specific design choice, affect construction safety generally in the form of predictability and continuity. As the worksite changes, workers often have difficulty anticipating and responding to change, which has been shown to affect safety to a great extent (Hanna, et al., 1999a, b; Kaming, et al., 1997; Thomas & Napolitan, 1995). Future researchers may continue exploring these constructs by adding clarity, external validity or by challenging our position.

The position of this research within past research and theory is shown in Figure 1. This figure shows how this research potentially offers empirical underpinning to existing theory, elucidating the relationships between objective indicators. The key addition in objective evidence to support observation and logical propositions.

The new knowledge gained through this inquiry has practical implications. In addition to constructability reviews that focus on specific design features and assemblies, a connection between RFIs and/or COs on safety may indicate that 1) reviews of potential design changes that would result in COs could be performed so that contractors could better anticipate and respond to potential change; and 2) the contractor's review of the design documents for clarity and completeness may reduce the frequency and scope of RFIs. Further, practitioners may recognize the potential negative implications of change orders and weigh the need for the change against the potential negative implications for safety.

Research Methods

To test the hypotheses and answer the associated research questions we implemented a two-phase research process. We adopted a mixed-methods approach, combining quantitative empirical data and qualitative data from interviews. This approach allowed us to explore if a connection between the variables of interest exists via statistical testing of empirical project data and explain why a connection exists, if one is observed, via interviews with experienced professionals. This combination adds richness that begins to allow for causal inference with suitable data and replication.

Phase 1. During the first phase, we gathered project demographic information, safety performance indicators, and design fidelity measures from a sample of 20 active or recently completed projects. We limited projects to design-bid-build (DBB) because the dynamics of COs and RFIs are not comparable among projects with different project delivery methods as previously discussed. All of the demographic and empirical data were collected either over the phone or via email from the project manager.

The demographic data included project location, scope (i.e., U.S. dollars), worker-hours accumulated at the time of interview, delivery method, contract method, and project type. The safety measures included the number of first aid injuries and number of OSHA recordable injuries. It should be noted that first aid injuries were defined as those injuries that resulted from an exposure or event in the workplace and that required some first-aid treatment but no medical treatment. Recordable injuries were defined as those incidents that resulted from an exposure or event in the workplace and that required some type of medical treatment beyond first aid or any loss of consciousness. In addition, the rate of COs, worker-hours related to COs, costs of COs, and the rate of RFIs were collected for each project.

Demographic information was normalized to rates so that the values among projects could be compared. For example, the number of OSHA recordable injuries was divided by the worker-hours accumulated on the project then multiplying by 200,000 to obtain the standard OSHA recordable injury rate (i.e., recordable injuries per 200,000 worker-hours). Similarly, a change order rate was computed by dividing the cost of change orders by the number of worker-hours accumulated. The following six indicators of design fidelity and two indicators of safety were devised from the empirical data:

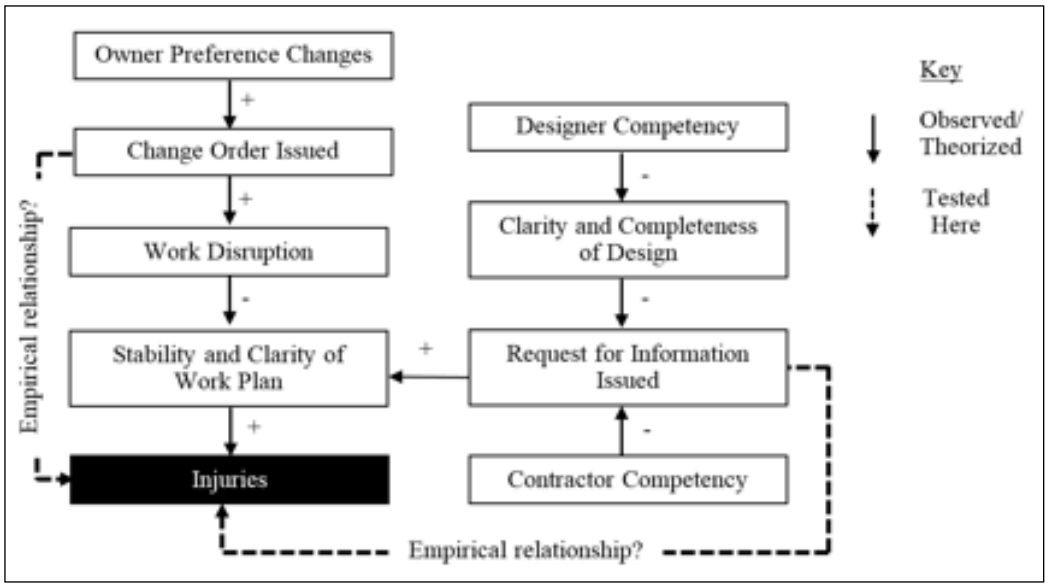

Figure 1: Theoretical relationships and position of this study.

•Cost of change orders per $1 million project scope completed (DF1),

•Cost of change orders per 200,000 worker hours (DF2),

•Number of worker hours related to change orders per $ 1 million project scope completed (DF3),

•Number of worker hours related to change orders per 200,000 worker hours (DF4),

•Number of RFIs per $ 1 million project scope completed (DF5), and

•Number of RFIs per 200,000 worker hours (DF6),

•Number of OSHA recordable injuries per 200,000 worker hours (INJ1), and

•Number of first aid injuries per 200,000 worker hours (INJ2).

Please note that the abbreviations used in the list above appear in the subsequent analyses and figures for clarity and precision.

The projects ranged in scope from $50,000 to $300 million and consisted of 15 U.S. and 5 projects outside the U.S. At the time of the interviews the worker-hours expended on the sample projects ranged from 160 to 1,081,600. The sample included 60% commercial, 15% residential, 10% institutional, 10% heavy civil and 5% industrial projects. Seventy percent used lump sum, 15% used cost plus contracts, 10% used unit price and 5% used negotiated contracts. The study sample consisted of both open-shop (70%) and union projects (30%). The construction work was in progress for eight projects that averaged 64% complete at the time of the study.

Project managers provided RFI, CO and safety data for all desired metrics on a project basis. The overall characteristics of the data include an average increase contract cost due to change orders of $205,007 with a standard deviation of $277,370; an average number of worker-hours related to change orders of 2,107 with a standard deviation of 3,745; and an average number of RFIs of 51 with a standard deviation of 70. The overall characteristics of the safety data include an average number of OSHA recordable injuries of 0.53 with a standard deviation of 1.45 and an average number of first-aid injuries of 4.24 with a standard deviation of 3.68. All of these values were converted into a rate per 200,000 worker-hours using the project demographics in the previous paragraph. Even though the sample size is relatively small, there was suitable variability in the demographics, CO, RFI and injury rates to perform robust statistical analyses.

Phase 2. The second phase of data collection consisted of open-ended interviews with 18 project management personnel. We collected the responses to the open-ended questions over the phone or in person. An important aspect of this process was that all interviews were performed with project managers from the same projects from which the empirical data from phase I were collected. This allowed us to use the qualitative responses to explain phenomena observed with the quantitative data. We did not collect data from safety managers because of their focus on safety performance. Instead, we desired project managers who have a more holistic set of project responsibilities.

The following basic, open-ended questions were asked in each interview:

	DF1	DF2	DF3	DF4	DF5	DF6	INJ1	INJ2
n	15	16	15	16	18	19	4	17
Mean	$29,946	$822,889	546	7,651	43.35	641	4.57	24.08
Min	$130	$1,405	1.18	27.74	0.06	3.21	0.36	0.29
Max	$149,796	$3,499,082	3,561	34,161	578	6,118	9.30	71.43
Range	$149,666	$3,497,677	3,560	34,134	57	6,114	8.95	71.14
St. Dev.	$47,549	$1,178,325	999	11,401	134	1,445	3.81	22.80

Table 1: Calculated indicator metrics and data distribution.

•What relationship, if any, exists between RFIs and safety performance?

•(if applicable) Why do you think this relationship exists?

•What relationship, if any, exists between COs and safety performance?

•(if applicable) Why do you think this relationship exists?

These questions were designed to avoid biasing or leading the project managers with the team's preconceived notions. The interviews were conducted as a conversation with the project manager and, when possible, we asked for anecdotes that helped to explain their perspectives. The results were rich responses that could be pattern matched across interviewees.

Results & Discussions

The main objective of the quantitative data analysis was to empirically test the aforementioned hypotheses. Once we obtained all the necessary data, the design fidelity indicators and safety indicators were calculated. The metrics and the data distribution are shown in Table 1. To compare data from different sized projects, we normalized raw values using worker-hours expended and total project scope.

To determine if a statistically significant relationship exists between safety and design fidelity, we regressed every combination of the design fidelity predictor variables and the metrics for safety performance as the response variables. We calculated the Pearson product moment correlation coefficient (Pearson-r) for each pairwise comparison to determine the magnitude (strong or weak) and direction (positive or negative) of the relationship. The Pearson-r can range in value from -1 to +1, with zero representing no correlation or relationship, +1 representing a strong positive correlation, and -1 representing a strong negative correlation (Cook & Weisberg, 2009).

Next, we calculated the coefficient of determination (r^2), which provides the significance of a relationship. This measures the proportion of variance in the response variable that is explained by the predictor through a linear relationship. We considered coefficient of determination values greater than 0.50 as significant as this means that 50% or more of the variance in the response variable is explained by the predictor through a linear relationship. Less than 0.50 means that most of the variance is unexplainable (Panik, 2009).

Finally, where a significant relationship was found to exist, further analyses were performed on the data to determine that the data is linear, homoscedastic (consistency in the variance), and can be

	INJ1/DF1	INJ1/DF2	INJ1/DF3	INJ1/DF4	INJ1/DF5	INJ1/DF6
n	4	4	4	4	4	4
r	0.464	0.284	0.907	0.920	0.900	0.918
r^2	0.216	0.081	0.823	0.846	0.810	0.844
p-value	0.536	0.716	0.093	0.080	0.099	0.082

Table 2: Correlation results for recordable injury rate indicator compared to the six design fidelity indicators.

represented by a normal distribution. Additionally, the model was assessed for outlier and influential observations. All results below were found to be acceptable in these further analyses.

The analysis allowed for a comparison of each of the safety performance indicators with each of the six design fidelity indictors. Table 2 shows the correlation results for recordable injury rates (INJ1) when compared to design fidelity indicators. This information indicates that there is a significant relationship between number of worker-hours expended to address change orders (DF3 and DF4) and recordable injuries. Also, there is a relationship between recordable injury rate and number of RFIs issued on a project (DF5 and DF6). However, a relationship was not found to exist between the recordable injury rate and the total cost of change orders (DF1 and DF2). Thus, the null hypotheses for H2 and H3 are rejected, while the null hypothesis for H1 is accepted for recordable injury rate.

In the four significant relationships the Pearson-r values were greater than 0.90, the coefficient of determination values were greater than 0.80 and the *p*-values were less than 0.10. In the two cases where no relationship was found, the r^2 values were all less than 0.50, with *p*-values of 0.536 and 0.716, respectively. In addition, the Pearson-r values for all four relationship cases are positive, which means that a positive correlation exists between recordable injury rates and design fidelity in terms of worker-hours expended to address change orders and the number of RFIs issued on a project.

For the second safety performance indicator, first-aid injury rate, the results of the correlation analysis did show a relationship between first-aid injuries and RFIs (reject H3 null hypothesis), but no relationship was found with first aid injuries and change orders (accept H1 and H2 null hypotheses). When reviewing the results in Table 3, one can see that the *p*-values for DF5 and DF6 are only suggestive, with an alpha of 0.10. These are both very weak correlations (r^2 are 0.175 and 0.176, respectively) and *p*-values that are close to the study alpha of 0.10. Therefore, the implication of these results is that while minor injuries may increase due to poor design fidelity, more severe injuries will increase.

Interestingly, the results related to COs can be interpreted to mean that the time required to address a change order is a factor related to safety but the cost of the change order is not. This makes sense in the context of disruption because the cost of the change order may not correspond directly to the level of disruption that it causes. For example, the replacement of a piece of laboratory equipment may be very expensive but, if the installation method is similar, the number of worker hours required to address this change may be very low. In this example, the change would not be very disruptive. In contrast, a change that requires a lot of worker-hours to address may not necessarily incur large costs and may be very disruptive. For example, if the client wishes to change the adjacent soil grading of a lot, there may not be a significant cost difference but the time and effort required to address the change could be significant. In this example, the change would be comparatively disruptive.

With respect to RFIs, the results indicate that, as the rate of RFIs increases, the recordable injury rate and first aid rate increases. This means that if design information is unclear and confusing, work may be less predictable and, thus, less safe. Previous research shows that working with distractions or in an unknown situation provides for a higher probability of an injury occurring (Hinze, 1997).

Interview Results

Data from the interviews show that the opinions of the relationship between design fidelity and construction safety performance confirm the quantitative results. When asked to explain why a relationship exists between COs and safety performance, one project manager summed the relationship well with the statement that "modifying the design can add a certain level of risk, especially to fast-paced projects. This causes serious changes to the work and the safety plan. Workers sometimes have a difficult time dealing with changes, especially when they are unexpected." Other project managers noted that, "COs cause frustration among the workers when they come at the last minute or during very busy times." When the workers have planned an activity and the owner/designer requests a change, the workers "do not put the same effort into replanning the safety of the process." Finally, COs are often requested in response to mistakes made early in design. According to one representative project manager, "COs are often a symptom of poor design where the design in general is hastily prepared. Such designs are difficult to construct and safety is rarely considered."

	INJ2/DF1	INJ2/DF2	INJ2/DF3	INJ2/DF4	*INJ2/DF5*	*INJ2/DF6*
n	14	15	14	15	16	17
r	0.129	0.156	0.111	0.153	0.418	0.419
r^2	0.017	0.024	0.012	0.023	0.175	0.176
p-value	0.660	0.580	0.705	0.586	0.107	0.094

Table 3: Correlation results for first aid injuries compared to the six design fidelity indicators.

Project managers were split in their perspectives of the impact of RFIs on safety. Although few noted that RFIs cause injuries and illnesses, they did believe that RFIs are a strong indicator of the clarity of design. Usually, the design is substantially complete with the exception of small errors, omissions, or inconsistencies among project documents (e.g., plans and specifications). These responses to RFIs typically do not have large impacts on the means and methods of construction; however, in some cases the responses require immediate changes that workers are not expecting. Finally, like COs, RFIs often are indicators of the quality and thoughtfulness of design. When many RFIs are required, the project managers felt that constructability was clearly not a priority for the client-designer team. All project managers felt that the level of constructability impacts construction safety implicitly.

Study Limitations

Although we used project data to test hypotheses formed from the existing body of knowledge and conducted interviews to obtain insight for the findings, there are some study limitations as noted below:

•The small sample size and lack of random sampling limits the ability to generalize the results to the entire construction industry. A major reason for this sample size was the reluctance of the contractors to provide data. We recommend further study with a larger number of projects.

•A disproportionate number of sample projects (47%) were built in Colorado. Interpreting the results may be skewed by the dominance of projects from one state. We suggest future research comprising a diversified pool of projects from several states.

•This research does not consider other safety interventions implemented by the contractor or the value of their safety program as a confounding factor.

•We considered RFIs and COs to be indicators of design. It has yet to be clearly established that these constructs are primarily design-related, although logic and the interview results indicate that this may be true.

Although these limitations must be addressed, this study has laid the foundations for future research that examines the relationship between safety and design fidelity.

Conclusion

Past researchers have reported some indirect links between design fidelity and safety performance through impacts on trade stacking, lowered employee morale, schedule compression, and work sequencing (Hanna, et al., 1999 a, b). However, none of the studies used empirical data to demonstrate a direct relationship between design fidelity and safety performance. Additionally, there is a plethora of publications describing methods and techniques that help to improve safety on construction projects (Gambatese, et al., 1997), yet there are no studies that directly relate design fidelity with safety performance. In fact, the field of PTD in construction is dominated by unsubstantiated theory with minimal empirical evidence.

To address this knowledge gap we studied the relationship between design fidelity and safety performance on DBB construction projects. We conclude that for DBB projects as the design fidelity increases on a project, the construction safety also tends to increase. However, as suggested by some project manager interviewees, there may be special cases where the contractor is capable of managing design uncertainty and changes. We recommend further study with a larger sample size and investigation of other project delivery methods such as DB and CM/GC.

Based on these conclusions, there are several immediate applications to the construction industry. We have found that increased design fidelity improves safety performance. This added benefit should provide an impetus to the project team to focus their efforts to increase design fidelity. Owners should take the lead and implement management strategies that will reduce the root causes of change orders and RFIs. For example, design errors and omissions typically cause change orders (Clarke, 1990). It is known that design errors/omissions and owner changes may result from poor project definition, inadequate pre-project planning, ineffective design, inadequate project change management, poor communication among owners, designers and constructors or lack of constructability reviews (CII, 2002). Management strategies should be developed to counter each explore relationships between design fidelity and safety performance. The results of this study indicate that there is a connection between the frequency of change orders and requests for information and safety performance, supported by both empirical data and the results of interviews with project managers. The implication is that efforts should be made to ensure that designs are of high enough quality that they can be easily interpreted by competent contractor and owners should be careful to note that their requested changes may have adverse impacts on construction safety.

We suggest that owners take a lead role in improving design fidelity by 1) ensuring changes are kept to a minimum during construction; 2) hiring designers who have low rates of RFIs; and 3) encouraging constructability reviews during design. Furthermore, selecting integrated or design-build project delivery is likely to improve design fidelity through enhanced up-front communication. Future researchers may wish to build upon this work by investigating the relationship between design fidelity and other project outcomes, exploring the root causes of design change and instability, investigating design fidelity after a major incident occurs, and understanding the types of instable work that most impact safety. ■

Acknowledgments

The authors would like to thank all the companies that participated in this study and provided project data.

References

Alnuaimi, A.S., Taha, R.A., Mohsin, M.A., & Al-Harthi, A.S. (2010). Causes, rffects, benefits and remedies of change orders on public construction projects in Oman. *Journal of Construction Engineering and Management, 136*(5), 615-622.

American Institute of Architects. (1977). General conditions of the contract for construction. AIA document A201. Washington, DC: Author.

Anderson, S., Fisher, D., & Rahman, S. (2000). Integrating constructability into project development: A process approach. *Journal of Construction Engineering Management, 126*(2), 81-88.

Behm, M.G. (2005). Linking construction fatalities to the design for construction safety concept. *Safety Science, 43,* 589-611.

Behm, M.G. (2009, Oct.). Employee morale: Examining the link to occupational safety and health. *Professional Safety, xx*(10), 42-49.

Behm, M. & Culvenor J. (2011). Safe design in construction: Perceptions of engineers in Western Australia. *Journal of Health & Safety Research & Practice 3*(1), 9-32.

Bureau of Labor Statistics (BLS) (2011). Census of fatal occupational injuries summary, 2010 [Economic News Release]. Retrieved from http://www.bls.gov/news.release/cfoi.nr0.htm

Esmaeili, B. & Hallowell, M.R. (2012). Diffusion of safety innovations in the construction industry. *Journal of Construction Engineering and Management, 133*(8), 955-963.

Christensen, W. C. (2011, April). Prevention through fesign: Long-term benefits. Retrieved from www.asse.org/assets/1/7/1104Christensen_interview.pdf

Cook, R. D., & Weisberg, S. (1999). *Applied regression including computing and graphics.* New York, NY: John Wiley & Sons.

Construction Industry Institute (CII). (2002, July). CII best practices guide: Improving project performance (IR 166-3). Austin, TX: University of Texas at Austin.

CII. (1986, July). Constructability: A primer (Publication 3-1). Austin, TX: University of Texas at Austin.

Francis, V.E., Chen, S.E., Mehrtens. V.M., et al. (1999). Constructability strategy for improved project performance. *Architectural Science Review, 42*(2), 133-138.

Gambatese, J. (1998). Liability in designing for construction worker safety. *Journal of Architectural Engineering, 4*(3), 107-112.

Gambatese, J. (2000). Safety constructability: Designer involvement in construction site safety. In K.D. Walsh (Ed.), *Construction Congress VI: Building Together for a Better Tomorrow in an Increasingly Complex World*. Reston, VA: American Society of Civil Engineers

Gambatese, J. (2004). An overview of design-for-safety tools and technologies. In S. Hecker, J. Gambatese & M. Weinstein (Eds.), *Designing for safety and health in construction: A research and practice symposium,* pp. 109-117. Portland, OR: University of Oregon Press.

Gambatese, J. Behm, M. & Hinze, J (2005). Viability for construction worker safety. *Journal of Construction Engineering Management, 131*(9), 1029-1036.

Gambatese, J.A., Hinze, J. & Hass, C.T. (1997). Tool to design for construction worker safety. *Journal of Architectural Engineering, 3*(1), 32-41.

Gambatese, J.A., Rajendran, S. & Behm, M.G. (2007). Green design and construction: Understanding the effects on construction worker safety and health. *Professional Safety, 52*(5), 28-35.

Hanna, A.S., Camlic, R., Peterson, P.A. & Nordheim, E.V. (2002). Quantitative definition of project impacted by change orders. *Journal of construction engineering Management. 128*(1), 57-64.

Hanna, A.S., Russell, J.S., Gotzion, T.W. & Nordheim, E.V. (1999a). Impact of change orders on labor efficiency for mechanical construction. *Journal of Construction Engineering and Management, 125*(3), 176-184.

Hanna, A.S., Russell, J.S. & Vandenberg, P.J. (1999b). The impact of change orders on mechanical construction labor efficiency. *Construction Management and Economics, 17*(6), 721-730.

Hanna, A., Tadt, E. & Whited, G. (2012). Request for information: Benchmarks and metrics for major highway projects. J*ournal of construction engineering Management, 138*(12): 1347-1352. doi 10.1061/(ASCE)CO.1943-7862.0000554

Hinze, J. (1997). *Construction safety.* Upper Saddle River, NJ: Prentice Hall.

Hinze, J. (2000). Designing for the life cycle safety of facilities. Paper presented at the Designing for Safety and Health Conference, sponsored by C.I.B. Working Commission W99 and the European Construction Institute, London, U.K.

Hinze, J. (2003). The owner's role in construction safety (Construction Industry Institute Research Summary 190-1). Austin, TX: The University of Texas at Austin.

Hinze, J. & Gambatese, J.A. (2003). Factors that influence safety performances of specialty contractors. *Journal of Construction Engineering Management, 129*(2), 159-164

Hinze, J. & Gambatese, J.(1996). Addressing construction worker safety in the project design (Construction Industry Institute Research Report 101-11). Austin, TX: The University of Texas at Austin.

Hinze, J., Mathis, J., Frey, P.D., Wilson, G., et al. (2001). Making zero accidents a reality: Annual conference of the Construction Industry Institute, San Francisco, CA.

Hinze, J.W. & Wiegand, F. (1992). Role of designers in construction worker safety. *Journal of Construction Engineering and Management, ASCE, 118*(4), 677-684.

Ibbs, C.W. (1997). Quantitative impacts of project change: Size issues. *Journal of Construction Engineering and Management, 123*(3), 308-311.

Kaming, P., Olomlaiye, P., Holt, G. & Harris, F. (1997). Factors influencing construction time and cost overruns on high-rise projects in Indonesia. *Construction Management and Economics, 15,* 83-94.

Mohamed, S., Tilley, P.A. & Tucker, S.N. (1999). Quantifying the time and cost associated with the request for information (RFI) process in construction. *International Journal of Construction Information Technology 7*(1), 35-50.

National Safety Council. (2011). *Injury facts, 2011 edition*. Itasca, IL: Author.

Panik, M. (2009). *Regression modeling.* Boca Raton, FL: Taylor & Francis Group.

Perkins, R.A. (2007). Sources of changes in design/build contracts for a governmental owner, management of engineering and technology. *Portland International Centre for Publication, 5-9,* 2148-2153.

Rajendran, S. (2006). *Sustainable construction safety and health rating system* (Doctoral dissertation). Oregon State University, Corvallis, OR. Retrieved from https://ir.library.oregonstate.edu/xmlui/handle/1957/3805

Stocks, S.N. & Singh, A. (1997). Studies on the impact of functional analysis concept design on reduction in change orders. *Construction Management and Economics, 17,* 251-267.

Szymberski, R. (1997). Construction project safety planning. *TAPPI Journal, 80*(11), 69-74.

Thomas, H.R. & Napolitan, C.L. (1995). Quantitative effects of construction changes on labor productivity. *Journal of Construction Engineering and Management, 121*(3), 290-296.

Toole, T.M. (2005). Increasing engineers' role in construction safety: Opportunities and barriers. *Journal of Professional Issues in Engineering and Education Practice, 131*(3), 199-207.

Toole, T.M. & Gabrielle, C. (2012). Prevention through design as a path toward social sustainability. *Journal of Architectural Engineering, 19*(3), 169-173. doi 10.1061/(ASCE)AE.1943-5568.0000107

Toole, M. & Marquis, S. (2004). Site safety attitudes of U.S. and U.K. design engineers. In S. Hecker, J. Gambatese & M. Weinstein (Eds.), *Designing for safety and health in construction: A research and practice symposium.* Eugene, OR: University of Oregon Press.

Wu, C., Hsieh, T. & Cheng, W. (2005). Statistical analysis of causes for design change in highway construction in Taiwan. *International Journal of Project Management, 23*(7), 554-563.

Impact of Discretionary Safety Funding on Construction Safety

Siyuan Song, Ibukun Awolusi and Eric Marks

Abstract

The U.S. construction industry continues to be plagued by workplace injuries, illnesses and fatalities. Many construction companies choose to invest more in safety (discretionary safety funding) than required by safety regulatory agencies. The objective of this research is to explore the correlation between a construction company's discretionary safety funding strategy and its safety record. This includes an investigation of individual categories of safety discretionary funding and how they impact a company's safety performance. Companies licensed as civil and heavy construction in the U.S. were interviewed about their safety record and safety discretionary funding. Results indicate that increasing discretionary safety funding can improve a company's safety performance. These results suggest that construction companies can promote safety on their projects by investing in specific categories of discretionary safety funding including training and technology.

Keywords

safety, discretionary spending, construction costs, construction companies, management

The U.S. construction industry continues to be plagued by workplace injuries, illnesses and fatalities. Governmental agencies, such as OSHA (2017) established regulations requiring construction companies to provide a specific level of safety for their employees. These safety regulations require construction companies to invest in safety to provide mandatory personal protective equipment, safety training and to satisfy other regulations. Some construction companies choose to invest more funding in an attempt to promote safety beyond OSHA regulations (Arditi et al. 2000).

For the purposes of this research, this type of funding is defined as *safety discretionary funding.* The research explores how safety discretionary funding of construction companies impacts their safety performance. Specific categories of safety discretionary funding are investigated to understand their effectiveness when mitigating injuries and fatalities within a specific construction company.

Literature Review

The construction industry continues to rank as one of the most hazardous work environments when compared to other industrial sectors in the U.S. (BLS, 2017a). Several industry and research efforts have been made to improve the safety record of the construction industry (Ameyay, et al., 2016; Aminbakhsh, et al., 2013, Cohn & Wardlaw, 2016). This section reviews current construction industry and fatality incidents. The review also discusses safety best practices of the construction industry and construction safety research efforts. A literature map containing identified related fields in construction safety is presented. Based on the findings of the review, a research needs statement is derived.

Construction Safety & Cost Statistics

U.S. employment statistics indicate that the construction industry accounted for approximately 19% of the nation's workplace fatalities, but only employs 5% of the nation's workforce (BLS, 2017a, b). In 2015, Bureau of Labor Statistics (BLS) reported 924 fatalities in the construction industry which was a decreased value from the 902 fatalities reported in 2014 (BLS, 2017a). Although fatalities are the worst-case scenario in construction safety, injuries and illnesses also present safety concerns for the construction industry. Construction industry personnel experienced 199,600 injuries in 2015 and 196,300 injuries in 2008 (BLS, 2017d).

The combined cost of fatal and nonfatal injuries in the U.S. construction industry was estimated to be $11.5 billion per year (Waehrer, 2009). The average cost per incident including fatal and nonfatal was estimated to be $27,000 (Waehrer, 2009). The study also identified the average injury compensation payment for a construction worker was $7,542 which is nearly double the average injury compensation for an employee in other industrial sectors (Waehrer, 2009).

Siyuan Song is a Ph.D. student at the University of Alabama in the Department of Civil, Construction and Environmental Engineering and previously obtained a master's degree from the same university. Siyuan specializes in creating user interfaces and corresponding applications in building information modeling (BIM) in an attempt to support safety management personnel on construction sites.

Ibukun Awolusi is a Ph.D. student at the University of Alabama in the Department of Civil, Construction and Environmental Engineering. He previously obtained a master's degree from the University of Alabama. Ibukun's research focus is in automated sensing of construction resources and hazards as well as collecting and analyzing safety leading indicators.

Eric Marks, Ph.D., P.E., is an assistant professor at the University of Alabama in the Department of Civil, Construction and Environmental Engineering. His research focuses on creating and leveraging technology, innovation and information to enhance safety performance on construction sites. He may be reached at eric.marks@eng.ua.edu.

Construction Safety Best Practices

Per OSHA regulations, construction companies are required to provide a work environment free of recognized hazards and be compliant with all the current regulations and standards for safety (OSHA, 2012). Many components of this regulation require funding by the construction company including providing personal protective equipment for workers, recording injuries, illnesses and fatalities and training all employees in proper safety procedures. Other safety funding such as creating a safety culture within the company and implementing new safety technologies are not required by OSHA and thus are at the discretion of the construction company. For the purposes of this research, this type of funding is defined as discretionary safety funding.

Technology Implementation

One category of discretionary safety funding used by many construction companies is technology implementation; however the construction industry has historically been slow to implement new innovation and technology (Peansupap & Walker, 2005). Researchers have attempted to implement technology to improve safety in construction (Cheng & Teizer, 2013; Hadikusumo & Rowlinson, 2004; Li, et al., 2009).

One study investigated the cost and benefits of implementing information technology in the construction industry (Love, 2005). The study identified a major barrier for implementing information technology in the construction industry is the lack of a specific vision for technology (Love, 2005). The study also identified that construction companies either exclude or inaccurately calculate indirect cost when comparing the cost of benefits of implementing information technology (Love, 2005). Different construction companies significantly differ in the amount they invest for information technology and these investment level decisions were not necessarily influenced by organizational size (Love, 2005). The study also found that many construction organizations often do not implement a methodology for making decisions to invest in information technology (Love, 2005).

Implementation of new information technology has often resulted in delays and costly problems for firms (Harty, 2005). Most construction firms do not undertake any form of financial evaluation of their technology investment (Love , 2004). Of companies that use financial analysis, discounted cash flow methods are the primary financial tool used by construction companies to assess their safety technology investments (Love, 2004). No significant differences in information technology investments exists with regard to firm size and approach to evaluating their information technology investments (Love, 2004).

Safety Culture & Climate

A link has been identified between construction companies investing in safety climate and an experienced performance in safety performance (Clarke, 2006; Mohamed, 2002; Molenaar, 2009). Safety culture was defined as the product of individual and group values, attitudes, perceptions, competencies and patterns of behaviour that determine the commitment to and the style and proficiency of an organization's safety and health management (Choudhry, 2007).

Construction companies often use discretionary safety funding to influence their employees' attitudes and behavior in relation to an organization's ongoing safety and health performance (Choudhry, et al., 2006). One study implemented meta-analysis to examine criterion-related validity of the relationships between safety climate, safety performance and occupational incidents and injuries (Choudhry, et al., 2006). The relationship between safety climate and incident involvement was found to be moderated by the study design in which incidents were measured following the measurement of safety climate, demonstrated validity generalization (Choudhry, et al., 2006). The study is limited to the size and function of the created model and the study failed to discuss investment costs of implementing a safety culture (Choudhry, et al., 2006).

Management Commitment

Researchers have suggested that reactive safety costs (costs incurred after an incident or fatality) may be minimized or avoided through focused safety efforts on construction jobsites (Abudayyeh, et al., 2006). A correlation was identified between management's commitment to safety and the frequency of construction-related injuries and illnesses (Pinion, et al., 2017). The largest indicator of a management's commitment to safety is the investments made for safety including discretionary safety funding (Abudayyeh, et al., 2006). The owner has a significant responsibility with safety on a construction site (Huang & Hinze, 2006). A relationship was identified between project safety performance and the owner's influence on safety (Huang & Hinze, 2006).

Design for Safety

Other forms of discretionary safety funding include designing construction equipment, materials and site layouts for safety (Zhu, et al., 2016). Safety design decisions made upstream from the construction job site can influence construction worker safety (Tymvios & Gambatese, 2016). One study analysed more than 200 fatality investigation reports and identified a significant correlation between construction design and safety (Behm, 2005). More specifically, 42% of the fatalities reviewed were linked to the design concept (Behm, 2005). Although the study linked construction safety to design concepts, the researcher was unable to identify specific design elements that impact construction safety (Behm, 2005).

Research Needs Statement

Safety discretionary funding has demonstrated its ability to improve the safety performance of a construction company. Further examination is needed to understand which categories of safety discretionary funding can maximize a company's safety performance. A research need exists to evaluate how investing in a specific category of safety discretionary funding impacts the company's safety record and how workplace safety is impacted by safety discretionary funding. The literature review is summarized in Figure 1 (p. 380) using a literature map. The need for safety discretionary funding is identified in Figure 1.

Research Objective & Scope

The goal of this research is to promote construction safety

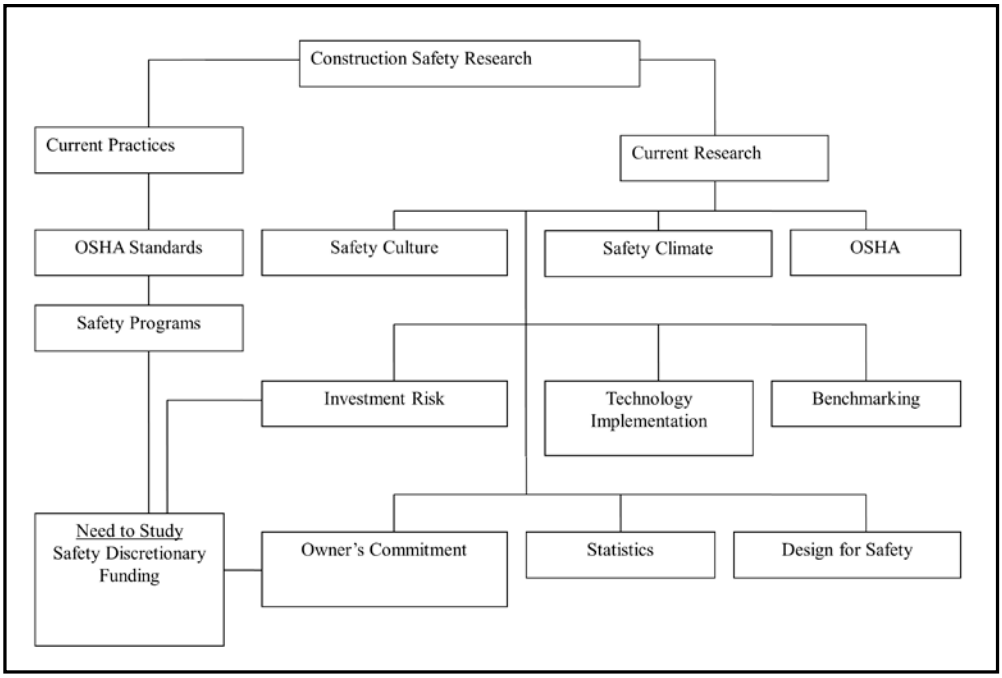

Figure 1: Construction safety literature map.

performance in an attempt to better understand the impact of discretionary safety funding on construction safety. The following two objectives were instituted to accomplish the stated research goal: 1) identify methods used by construction companies to make decisions about safety discretionary funding; and 2) test a correlation between a construction company's safety funding strategy and its safety record. The research is limited to construction companies in the U.S. that have an established safety program. The companies are under the jurisdiction of OSHA and other U.S. government organizations regulating safety in the workplace.

Research Methodology

The workflow for this research was divided into three sequential processes: 1) participant selection; 2) survey tool; and 3) data analysis. The workflow created a survey from the identified variables and distributed the survey to selected participants. Data gathered from the survey was analysed and evaluated.

A mixed methods research approach was used to execute this research with most of the research being categorized as quantitative. The independent variables included the number of injuries, illnesses and fatalities of company employees as well as the size of the construction company. The dependent variables were defined as the percentage invested per year in each category of safety discretionary funding.

Participant Selection

Participants of this research were safety directors of construction companies performing heavy and civil projects. A survey sample size determination equation was used to determine a sample size of 50 participants based on an estimated 10% response rate and 95% confidence interval (Bernard, 2000; Fowler, 2002).

A random sampling generator function was used to determine which companies would be solicited for participation in the study. The 50 numbers randomly generated were assigned to company listing numbers in the top 400 contractors list provided by the *Engineering News Record* in 2014 (ENR, 2014). Each of the selected company numbers were contacted and invited to participate in the survey. Safety directors who agreed to participate in the research were assured that all company proprietary information (all statistics) would remain anonymous and that the research results would be delivered to all participants. Of the 55 companies invited to participate, 23 companies showed interest in the research and 10 companies completed the survey.

Survey

The surveys were distributed by e-mail to the 10 construction companies that agreed to participate in the research. The survey was divided into two sections: company safety statistics and discretionary safety funding. The company safety statistics section covers the current and past safety information of the company, specifically the record of injuries, illnesses and fatalities per year from 2002 to 2011. The second section surveyed the current and past discretionary safety funding information of the company. Participants are asked to provide an estimate of the percentage of discretionary safety funding per year from 2002 to 2011. The survey also asks participants to list the top five discretionary safety categories they invested in on average from 2002 to 2011. Open response questions were included in the second section to allow participants to express other opinions not covered in the survey.

Data Analysis

Each participating construction company had a different number of employees, active projects, safety program strategies and employee work hours. A variety of techniques were implemented for data analysis. The safety incident rate prescribed by OSHA was used to compare and contrast injury, illness and fatality data between surveyed companies. This rate standardizes the number of cases by a ratio of company employee hours and an average company's employee hours (BLS, 2017a). Because the safety discretionary funding values were given as a percentage of the total discretionary safety budget, the impact of company size and spending patterns were decreased when comparing values of different companies.

Surveyed companies with the lowest and highest incident rates were particularly interesting because their discretionary safety funding categories represented the best- and worst-case scenarios. Companies that showed either an increase or decrease in overall discretionary safety funding were also used to understand the impact of safety discretionary funding on a company's incident record over time.

Cronbach's alpha was used as the reliability measurement method for information obtained from the survey (Stanos, 1999). Participants of the survey were asked to respond to a follow-up question 7 days after they completed the survey. The follow-up question asked each company the number of injuries and illnesses in 2004 and this number was compared to the initial value given. Cronbach's alpha values higher than 0.7 are deemed to be reliable survey results. The Cronbach's alpha from this survey was 0.89.

Results & Discussion

Information obtained from the 10 surveyed construction companies was analysed and used to achieve the stated research objectives. Companies that boasted the lowest incident rates were compared to others to track the amount invested in discretionary safety funding. Companies that demonstrated an increase or decrease over time in discretionary safety funding were also compared with others with regard to their incident rate. Specific categories of discretionary safety funding were also evaluated to find how the category impacted the safety incident record of a company. Lastly, selected statements from the open response section are included in this section.

Company	Range of Injuries per Year		Range of Fatalities per Year	
	Maximum	Minimum	Maximum	Minimum
1	0	25	0	0
2	0	21	0	1
3	0	20	0	1
4	5	40	0	2
5	5	42	0	0
6	6	30	0	0
7	8	32	0	0
8	0	42	0	1
9	8	31	0	0
10	0	19	0	0

Table 1: Yearly injury and fatality ranges of interviewed construction companies.

Company	Technology	Training	Program	Research	Equipment	Incentives
1	10	25	5	0	60	0
2	0	85	5	0	10	0
3	25	50	10	5	10	0
4	0	25	60	5	5	0
5	0	65	15	0	5	5
6	0	30	10	15	20	0
7	0	25	10	10	15	5
8	25	70	0	0	2	50
9	3	10	0	0	0	25
10	5	20	40	3	5	25

Table 2: Percent of yearly spending per company for safety discretionary spending categories.

Company Safety Statistics

Although the fatality information was available for each company between the years of 2002 and 2011, only the injury and fatality data were used for evaluation. Recorded injuries and illnesses provide insight to poor or absence safety performance within a construction company. The number of employees for each of the construction companies ranged from 75 to 2,000. The range of annual revenues of the interviewed companies is $20 million to $5 billion. Eight of the interviewees from the companies were safety directors and the other two were presidents of their respective companies. The services provided by the construction companies interviewed included engineering, fabrication and construction. Table 1 provides the range of injuries and fatalities per year for the interviewed companies

The three companies with the lowest incident rate over the 9-year period invested the largest portion of discretionary safety funding in new technology, additional safety program funding and additional safety training. The three companies with the highest incident rate over the 9-year period invested the largest portion of discretionary safety funding in employee incentives.

Discretionary Safety Funding

Specific categories of discretionary safety funding were also evaluated to find how the category impacted the safety incident record of a company. Categories of discretionary safety funding in which the surveyed companies invested include: technology, training, safety program, research, equipment and incentives. During the time period surveyed, the top three categories invested by the companies were safety training, safety program and employee incentives. The average percentage spent on the top three categories per company is listed in parenthesis: safety training (42.8%), safety program (17.2%) and employee incentives (15.7%).

Companies that demonstrated an increase or decrease over time in discretionary safety funding were also compared with others with regard to their incident rate. Three companies showed a gradual increase of safety discretionary funding between 2002 and 2011, and two companies decreased their amount of safety discretionary funding during the same time period.

Companies that increased their discretionary safety funding also experienced a decrease in their incident rate over the same time period. Companies that increased their safety discretionary funding invested in the following categories: safety program, safety training and employee incentives. Companies that decreased their safety discretionary funding invested in the following categories: additional safety equipment and safety training.

Open Response Questions

Apart from the construction safety statistics and discretionary safety funding percentages, the surveyed companies were asked to provide open-ended responses to three questions. The companies were first asked to name specific categories of discretionary safety investments they felt provided a great safety benefit to their company. One company indicated that investing in a company-wide wellness program including training for safety and health best practices provided an improvement in their com-

		Average OSHA TRIR (over 10yrs)	Average Number of Injuries (over 10yrs)
Average Percentage of Discretionary Safety Budget (over 10yrs)	Pearson Correlation	-.678*	
	Sig. (2-tailed)	.022	
	N	10	
Number of Employees	Pearson Correlation		.890**
	Sig. (2-tailed)		.000
	N		10

** Correlation is significant at the 0.01 level (2-tailed)
* Correlation is significant at the 0.05 level (2-tailed)

Table 3: Correlation of discretionary safety budget and company safety statistics.

		OSHA TRIR (Average of 10 Companies)	Percentage of Discretionary Safety Budget (Average of 10 Companies)
Year	Pearson Correlation	.669*	.913**
	Sig. (2-tailed)	.034	.000
	N	10	10

** Correlation is significant at the 0.01 level (2-tailed)
* Correlation is significant at the 0.05 level (2-tailed)

Table 4: Correlation impact of time on discretionary budget and company safety statistics.

pany's safety program. Other companies discussed their success with employee training programs including biannual safety seminars and professional development for safety personnel. Positive safety incentives for workers were also cited as investments that improved a company's safety program. These incentives included employee incentive programs, jobsite safety awards, family lunches, and others.

Survey participants were also asked to provide examples of discretionary safety investments that did not provide a great benefit for their company. The majority of responses discussed negative effects of providing employees with incentives. These negative impacts included not reporting incidents and lack of accountability for the incentive program. One company indicated that many new incentive competitions gradually transform into an expectation for the employees. Other responses indicated that accountability of an employee incentive program is a major factor in the success or failure of the program.

Many of the surveyed companies also chose to share additional feedback they felt was applicable to this research. One company indicated that an investment in safety technology was very complicated, but very beneficial. The response cited technology implementation as a major obstacle. Other companies supported the theory that discretionary safety investments in front-line management was vital to conduct construction operations in a safe manner.

Discretionary Safety Budget & Company Safety Statistics

Table 1 presents the correlation between the percentage of discretionary budget allocated for safety and the company's safety statistics. The percentage of discretionary safety budget of 10 construction companies over 10 years (i.e., from 2002 to 2011) was correlated with the companies' OSHA total recordable incident rate (TRIR). The value of the Pearson's correlation coefficient (r) of -0.678 shows that there is a strong negative correlation between the percentage of discretionary safety budget and the OSHA TRIR. The sig. (2-tailed) value of 0.022 also shows that the correlation between the two variables is significant at the 0.005 level. These results indicate that there is tendency for recordable injury rate to increase if the amount of funds allotted for safety management is reduced. This result is realistic in the sense that lack of adequate funding for the development and implementation of appropriate safety management practices and programs can increase the rate at which injuries occur on a construction site. This implies that a major aspect of safety management is the company's ability to appropriately fund the various practices and programs such as application of technology, safety training and research to mitigate injuries on construction sites.

The results in Table 3 also show that the number of employees that work on a construction site or project also impacts the number of injuries that occur on the site. The results of the analysis indicate that there is a very strong correlation between the two variables with a Pearson's correlation coefficient of 0.890 which is significant at the 0.001 level (2-tailed) with a p-value of 0.000. These results show that the number of injuries experienced on a typical construction site has a high tendency to increase as the number of workers is increased. A good way to put this issue under control will be to appropriate adequate funding for safety management to properly manage the high workforce thereby mitigating the possibility of having a heightened injury level on the construction site.

Impact of Time on Discretionary Safety Budget & Company Safety Statistics

Table 2 (p. 381) depicts the impact of time on the OSHA TRIR and the percentage of discretionary safety budget for 10 construction companies. The Pearson's correlation coefficient of 0.669 indicates that the injury rate for the 10 construction companies surveyed increased from 2002 to 2011 and that the correlation over those years is significant at the 0.05 level (2-tailed). The results also show that a very strong correlation exists between time and the discretionary safety budget with a correlation coeffi-

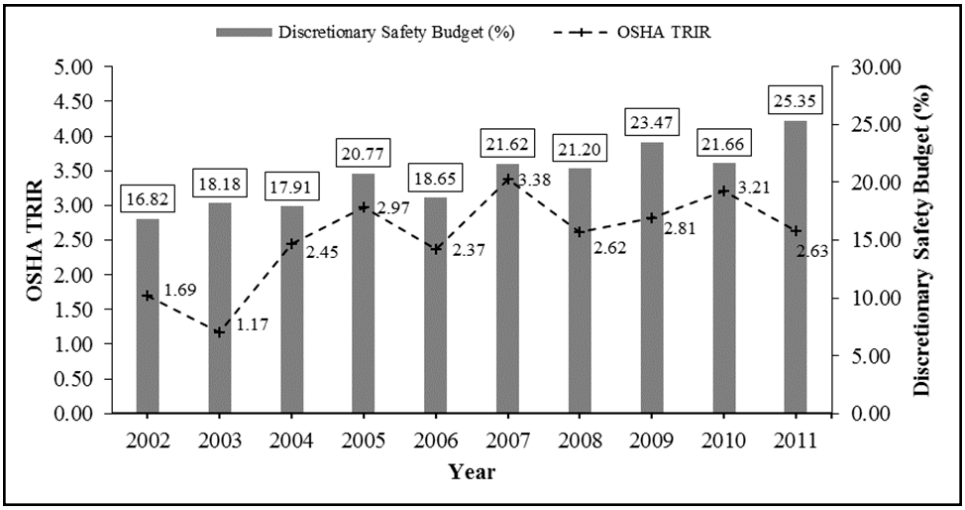

Figure 2: Periodic distribution discretionary budget and company safety statistics.

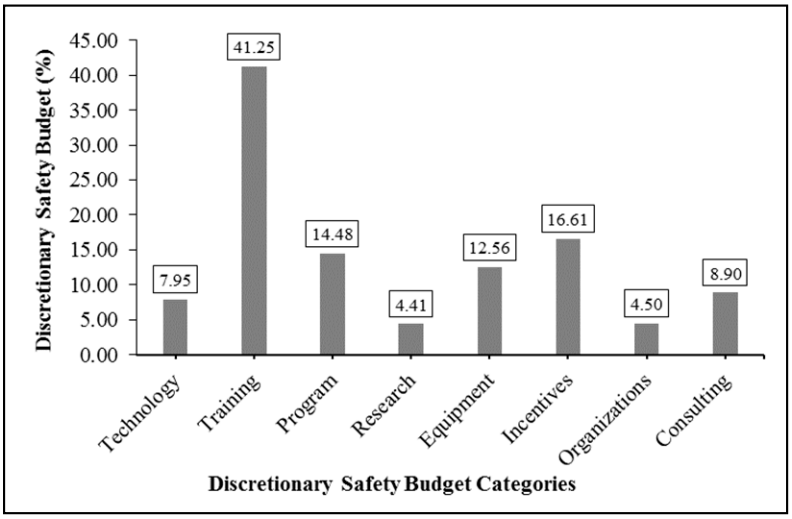

Figure 3: Discretionary safety budget categories.

cient of 0.913 significant at the 0.001 level (2-tailed) with p-value of 0.000. This implies that the percentage of budget allocated for safety has increased between 2002 to 2011 but this increase has not brought about a corresponding decrease in the OSHA TRIR and the number of injuries recorded. Apart from the fact that other factors may be responsible for these results, it could also be that the margin of increase in the budget over those years has not been commensurate or adequate enough to meet up with the ever-changing complexities of the construction processes which have a lot of impacts on safety. The distribution of how discretionary safety budget changed over time and the corresponding effects on the companies OSHA TRIR is presented in Figure 2.

Discretionary Safety Budget Categories

Figure 2 illustrates the discretionary safety budget categories and the percentage of budget allocated to each category. It can be seen in the figure that majority of the companies appropriate the highest percentage of discretionary safety funding to training with least been allotted to research. More fund is also being apportioned to incentives and programs ahead of technology. The implementation of technology for the mitigation of injuries has not received a wide-spread adoption in the construction industry as it is in other major sectors such as sports, manufacturing, etc. This implies that the lack of a specific vision for technology identified by Love (2005) is still a major barrier impeding the implementation of information technology in the construction industry. Also, these results show that research which provides the framework and principles on which most of the other categories are based is currently underfunded.

Safety Funding Limitations

Table 5 shows the ranking of some of the factors hindering safety funding in the construction industry. The results of the survey indicate that misappropriation of funds ranks highest among the factors with a mean item score (MIS) of 3.25 followed by inadequate funding and lack of management commitment with mean item scores of 3.00 each. These results underpin Love (2005) findings about inaccurate calculation of the cost of implementing information technology to construction safety. The least limiting factor was found to be positive incentives with MIS of 2.63.

Conclusions

The construction industry continues to experience an elevated number of workplace injuries, illnesses and fatalities when compared to other industries in the U.S. Construction companies are attempting to lower incident rates by investing in various categories of discretionary safety funding. This research investigates the correlation between safety discretionary funding of construction companies and their corresponding safety record. A survey tool was used to gather information from safety directors from 10 construction companies in the U.S. Results from the research suggest that increasing the amount of discretionary safety funding in a construction company can improve their incident record. Furthermore, companies that invest in safety programs, training and employee incentives can improve their safety record.

The research identified some limitations of this work and

Safety Funding Limitations	Mean Item Score (MIS)	Rank
Misappropriation of Funding	3.25	1
Inadequate Funding	3.00	2
Management Commitment	3.00	3
Negative Incentives	2.89	4
Positive Incentives	2.63	5

Table 5: Safety funding limitations.

areas of future research. As noted, only construction companies listed on the top 400 contractor list of the Engineering News Record (ENR 2014). Further surveys could include companies not included on this list. Future research could also further investigate the safety records and financial implications of discretionary safety funding. Future work could also integrate the potential impact of factors not included in discretionary safety funding on a company's incident rate. Although the information gathered by the survey was deemed successful, the aforementioned barriers could potentially have an influence on the reported results. These barriers along with others require further investigation to better evaluate the impact of safety discretionary funding on construction safety. ■

References

Abudayyeh, O., Fredericks, T., Butt, S. & Shaar, A. (2006). An investigation of management's commitment to construction safety. *International Journal of Project Management, 24,* 167-174.

Ameyaw, E., Hu, Y., Shan, M., Chan, A., et al. (2016). Application of Delphi method in construction engineering and management research: a quantitative perspective. *Journal of Civil Engineering and Management, 22,* 991-1000.

Aminbakhsh, S., Gunduz, M., Sonmez, R. 2013. Safety risk assessment using analytic hierarchy process (AHP) during planning and budgeting of construction projects. *Journal of Safety Research, 46,* 99-105.

Arditi, D., Koksal, A. and Kale, S. (2000). Business failures in the construction industry. *Engineering Construction and Architectural Management, 7*(2), 120-132.

Bureau of Labor Statistics (BLS). (2017a). Census of fatal occupational injuries: Current and revised data. Retrieved from https://www.bls.gov/iif

BLS. (2017b): Industries at a glance: Construction: NAICS 23. Retrieved from https://www.bls.gov/iag/tgs/iag23.htm#workforce

BLS. (2017c). Industries at a glance: Heavy and civil engineering construction: NAICS 237. Retrieved from https://www.bls.gov/iag/tgs/iag237.htm

BLS. (2017d). Industry injury and illness data. Retrieved from https://www.bls.gov/iif/oshsum.htm#15Summary_News_Release

Behm, M. (2005). Linking construction fatalities to the design for construction safety concept. *Safety Science, 43,* 589-611.

Cheng, T., Teizer, J. (2013). Real-time resource location data collection and visualization technology for construction safety and activity monitoring applications. *Automation in Construction, 34,* 3-15.

Choudhry, R., Fang, D. & Mohamed, S. (2007). Developing a model of construction safety culture. *Journal of Management in Engineering, 23,* 207-212.

Choudhry, R., Fang, D. & Mohamed, S. (2006). The nature of safety culture: A survey of the state-of-the-art. *Safety Science, 45,* 993-1012.

Clarke, S. 2006. The relationship between safety climate and safety performance: A meta-analytic review. *Journal of Occupational Health Psychology, 11,* 315-327.

Cohn, J. & Wardlaw, M. 2016. Financing constraints and workplace safety. *Journal of Finance, 71,* 2017-2058.

Engineering News Record. (2014). The top 400 contractors. Retrieved from http://www.enr.com/Top_Lists/Top_Contractors1

Hadikusumo, B. & Rowlinson, S. (2004). Capturing safety knowledge using design-for-safety-process tool. *Journal of Construction Engineering and Management, 130,* 281-289.

Harty, C. (2005). Innovation in construction: A sociology of technology approach. *Building Research & Information, 33,* 512-522.

Huang, X. & Hinze, J. (2006). Owner's role in construction safety. *Journal of Construction Engineering and Management, 132,* 164-173.

Li, R., Man, Y. & Sun, W. (2009). Future motivation in construction safety knowledge sharing by means of information technology in Hong Kong. *Journal of Applied Economic Sciences, 9,* 457-472.

Love, P., Irani, Z. & Edwards, D. (2005). Researching the investment of information technology in construction: An examination of evaluation practices. *Automation in Construction, 14,* 569-582.

Love, P. & Irani, Z. (2004). An exploratory study of information technology evaluation and benefits management practices of SMEs in the construction industry. *Journal of Information and Management, 42,* 227-242.

Mohamed, S. (2002). Safety climate in construction site environments. *Journal of Construction Engineering and Management, 128,* 375-384.

Molenaar, K., Park, J. & Washington, S. (2009). Framework for measuring corporate safety culture and its impact on construction safety performance. *Journal of Construction Engineering and Management, 135,* 488-496.

OSHA. (2017). About OSHA. Retrieved from https://www.osha.gov/about.html

OSHA. (2009). Inspections within industry. Retrieved from http://www.osha.gov/pls/imis/industry.html

Peansupap, V. & Walker, D. (2005). Factors enabling information and communication technology diffusion and actual implementation in construction organizations. *Journal of Information Technology in Construction, 10,* 193-218.

Pinion, C., Brewer, S., Douphrate, D., Whitehead, L., et al. (2017). The impact of job control on employee perception of management commitment to safety. *Safety Science, 93,* 70-75.

Stanos, J. (1999). Cronbach's alpha: A tool for assessing the reliability of scales. *Journal of Extension, 37,* 1-5.

Toole, T. (2002). Construction site safety roles. *Journal of Construction Engineering and Management, 128,* 203-210.

Tymvios, N. & Gambatese, J. (2016). Direction for generating interest for design for construction worker safety: A Delphi study. J*ournal of Construction Engineering and Management, 142*(8). https://doi.org/10.1061/(ASCE)CO.1943-7862.0001134

Waehrer, G., Dong, X., Miller, T., Haile, E., et al. (2007). Costs of occupational injuries in construction in the United States. *National Institutes of Health Public Access, 39,* 1258-1266.

Zhu, A., Zedtwitz, M., Assimakopoulos, D. & Fernandes, K. (2016). The impact of organizational culture on concurrent engineering, design-for-safety, and product safety performance. *International Journal of Production Economics, 176,* 69-81.

Click here to view the survey used in this research.